

Perspectives of 2D Materials for Optoelectronic Integration

Junru An, Xingyu Zhao, Yanan Zhang, Mingxiu Liu, Jian Yuan, Xiaojuan Sun, Zhiyu Zhang, Bin Wang,* Shaojuan Li,* and Dabing Li*

2D materials show wide-ranging physical properties with their electronic bandgaps varying from zero to several electronvolts, offering a rich platform to explore novel electronic and optoelectronic functions. Notably, atomically thin 2D materials are well suited for integration in optoelectronic circuits, because of their ultrathin body, strong light–matter interactions, and compatibility with the current silicon photonic technology. In this paper, an overview of the state of the art of using 2D materials in optoelectronic devices and integration is provided. The optoelectronic properties of 2D materials and their typical electronic and optoelectronic applications including light sources, optical modulators, photodetectors, field-effect transistors, and logic circuits are summarized. The device configurations, operation mechanisms, and device figures-of-merit are introduced and discussed. By discussing the recent advances, future trends, and existing challenges of 2D materials and their optoelectronic devices, this review has provided an insight into the perspectives of 2D materials for optoelectronic integration and may guide the development of this field within the research community.

1. Introduction

Optoelectronic integration is beneficial for future mass data transmission, because the synergetic integration of electronic and optoelectronic components can achieve high bandwidth and high density I/O capabilities.^[1–4] With the dramatic increased demand of optoelectronic technology in recent years, achieving low cost, high speed, low energy consumption, and miniaturized optoelectronic devices is of great commercial and scientific interest. Although silicon optoelectronic technology

has been developed for many years, it remains a great challenge to fabricate all components in an optoelectronic system using silicon. III–V compound semiconductors (GaAs, GaN, InAs, etc.) have demonstrated very high carrier mobilities (9000 to $40\,000\text{ cm}^2\text{ V}^{-1}\text{ s}^{-1}$), and they have excellent performances in a variety of optoelectronic devices, such as high power electronic devices, light-emitting devices (LEDs), photodetectors, and so on. Optoelectronic integration based on III–V compound semiconductors was proposed in the 1980s, but due to its incompatibility with the current complementary metal-oxide-semiconductor transistor (CMOS) fabrication process, it has not been rapidly implemented in large-scale applications. Inspired by the photosynthesis in nature, the optoelectronic devices based on photosynthetic proteins and biomolecules, which can harvest solar energy, store it in chemical form,

and carry out the photochemical reactions with a quantum efficiency close to 100%, have also attracted much attention.^[5,6] The applications of these materials in optoelectronic devices have been demonstrated in solar cells, bio-sensors, photodetectors, etc.^[7–10] However, the limited lifetime of biomolecules and low overall efficiency of the reported devices have hindered their further development.

Recently, there have emerged many novel nanomaterials based optoelectronic devices with different functionalities, including LEDs, lasers, optical modulators, photodetectors,

J. An, X. Zhao, Y. Zhang, M. Liu, B. Wang, S. Li
State Key Laboratory of Applied Optics
Changchun Institute of Optics, Fine Mechanics and Physics
Chinese Academy of Sciences
Changchun, Jilin 130033, P. R. China
E-mail: binwang@ciomp.ac.cn; lishaojuan@ciomp.ac.cn

J. An, X. Zhao, Y. Zhang, M. Liu, B. Wang, S. Li, X. Sun, Z. Zhang, D. Li
University of Chinese Academy of Sciences (UCAS)
Beijing 100049, P. R. China

J. Yuan
School of Physics and Electronic Information
Huaibei Normal University
Huaibei, Anhui 235000, P. R. China

X. Sun, D. Li
State Key Laboratory of Luminescence and Applications
Changchun Institute of Optics, Fine Mechanics and Physics
Chinese Academy of Sciences
Changchun, Jilin 130033, P. R. China
E-mail: lidb@ciomp.ac.cn

Z. Zhang
Key Laboratory of Optical System Advanced Manufacturing Technology
Changchun Institute of Optics, Fine Mechanics and Physics
Chinese Academy of Sciences
Changchun, Jilin 130033, China

 The ORCID identification number(s) for the author(s) of this article can be found under <https://doi.org/10.1002/adfm.202110119>.

DOI: 10.1002/adfm.202110119

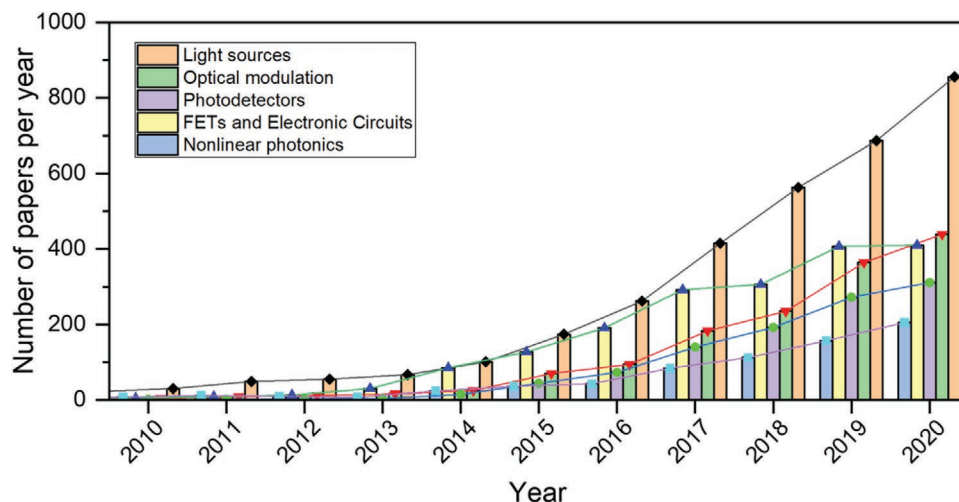


Figure 1. Number of papers published per year on various optoelectronic applications based on 2D materials in the past decade (data taken from ISI Web of Science). Solid lines are a guide for the eye illustrating the growth experienced by the volume of the literature.

field effect transistors (FETs), and so on.^[11–14] Among them, 2D materials have garnered enormous interest in optoelectronic integration due to their ultrathin body, strong light–matter interactions, and compatibility with the current silicon photonic technology. Their rich optoelectronic characteristics span light emission, optical modulation, saturable absorption, and electrically modulated field effect characteristics. Benefiting from these properties, substantial efforts have been devoted into 2D materials-based optoelectronic applications including light sources, optical modulators, photodetectors, FETs, and logic circuits. The number of publications per year in these fields increased dramatically in the past decade, as illustrated in **Figure 1**. A future goal is that these optoelectronic devices of different functional components move to the on-chip integration. To this end, integrating these devices with silicon becomes a viable solution, which means that existing CMOS fabrication process can be used to achieve low-cost manufacturing.

Vertical quantum confinement gets involved when the thickness of a material decreases down to the atomic-length scale, known as the 2D form of a material. Such transformation of a material from bulk to 2D planar leads to significant change in electronic or optical properties and also makes it possible to realize optoelectronic devices that can be scaled down to ultrasmall sizes. A stable planar 2D material were realized since the discovery of one-atomic-thick graphite (i.e., graphene) in 2004.^[15] The micromechanical exfoliation route was developed to exfoliate graphene from graphite and this approach was later found applicable to produce other 2D materials from their bulk counterparts.^[16] The fascinating properties of graphene has been revealed since then, including ballistic transport, tunable interband transition, linear dispersion of the Dirac electrons, frequency-independent light absorption across the spectrum, highly flexibility, and environmental stability.^[17,18] In addition to graphene, more 2D materials have been discovered afterward, such as layered transition metal dichalcogenides (TMDCs), black phosphorus (BP), 2D transition metal carbides, carbonitrides, nitrides (MXenes), and so on. Notably, 2D materials exhibit unique photoelectric properties, large

mechanical flexibility, and good compatibility with CMOS fabrication process, perfectly suited to the needs of optoelectronic integration. For instance, FETs and photodetectors based on different 2D materials have already been studied and shown good potential for applications.^[19,20] Meanwhile, 2D materials also demonstrate tunable optical response from the visible-to-infrared telecommunication band and mid-infrared (MIR) regions, demonstrating prospect in optoelectronic integration. Taking BP and PtSe₂ which have narrow bandgap as examples, they have been designed for infrared photonic devices such as photodetectors and optical modulators and exhibited impressive performances.^[21–23] Optical modulators based on graphene which has zero or gapless bandgap have been used for visible, infrared, and terahertz range successfully.^[24,25] Despite the atomic level of thickness, 2D TMDCs also show high light absorption, high carrier mobility at room temperature, and efficient light emission, providing a new platform for fabricating on-chip light sources.^[26] Especially, 2D materials represented by van der Waals-stacked heterojunctions and homojunctions possess small sizes, ultrathin thicknesses, easy processing, and novel physical phenomena for exploring optoelectronic applications.^[27–29] More importantly, optoelectronic devices based on 2D materials have been reported comparable performance at room temperature to devices based on traditional bulk semiconductors.^[30]

For optoelectronic integration, its basic functional units include light emission, optical modulation, light detection and reception, signal processing, and so on. In terms of these applications, 2D materials based integrated light sources, modulators, photodetectors, FETs, and logic circuits have all been realized.^[31,32] The introduction of 2D materials into integrated optoelectronics is not only the potential route to break through the limitations of existing silicon semiconductor technology, but also helpful to exploit novel applications in the future.

In this paper, we review the status and development of 2D materials based devices integrated with silicon. First, we begin with a brief introduction on the synthesis and optoelectronic properties of 2D materials and their heterostructures. Then,

we exemplify typical optoelectronic devices including 2D materials based light sources, optical modulators, and photodetectors, we also discuss the electronic properties of 2D materials, and review the development of 2D FETs and logic circuits. Following that, we summarize the development of integrated nonlinear photonics based on 2D materials before putting an emphasis on the integration of 2D materials with silicon planar photonics. Finally, the future opportunity and challenges in the optoelectronic integration are discussed.

2. Synthesis and Optoelectronic Properties of 2D Materials and Their Heterostructures

The integration of 2D materials into silicon optoelectronics will require the fabrication of large-scale, uniform, and highly crystalline 2D films, which is an on-going hotspot in the research field. Nowadays, there are generally two major methods of synthesizing and preparing 2D materials for optoelectronic devices, i.e., top-down methods and bottom-up methods. More specifically, top-down methods mainly include micromechanical exfoliation and liquid phase exfoliation methods,^[15,33–42] while bottom-up methods generally include chemical vapor deposition (CVD) and hydrothermal/solvothermal methods.^[43–53]

In earlier studies of 2D material, the preparation of 2D nanosheets for fundamental property investigation and functional device fabrication is highly relied on the micromechanical exfoliation.^[15] Because the in-plane chemical bonds in 2D materials are much stronger than the interlayer bonds, it is possible to exfoliating their bulk materials down to monolayer limits. Nevertheless, there are many variations using this method.^[33] The size and quality are limited by the dimensions and crystallinity of the source crystals. Furthermore, the low yield and poor throughput are big obstacles to real applications. Liquid phase exfoliation can be generally divided into “chemical exfoliation” and “direct liquid exfoliation” based on whether chemical reactions play a major role.^[35] Direct exfoliation methods can retain the original physical and electronic properties of the 2D materials. Generally, liquid phase exfoliation has low cost and relatively high yield in comparison with micromechanical exfoliation. Along with these, the produced 2D materials usually suffer from relatively small flake size. The hydrothermal/solvothermal method is another bottom-up way to synthesize 2D materials from heterogeneous/solvothermal reactions in aqueous media.^[53] But the generation of defects and formation of side products hinders its further application in electronic and optical devices.

Among the various methods for synthesizing 2D materials, CVD method has been successful used in large-scale fabrication of several representative 2D materials, such as graphene, hexagonal boron nitride (h-BN), and TMDCs.^[43–45,54–57] For the growth of graphene and h-BN, metals like Cu and Ni, are often used as promising catalyst, epitaxial substrate, or dissolution source of the reaction atoms.^[46,47] For the growth of TMDCs, precursors like transition metals (e.g., Mo, W, Pt, etc.), transition metal oxides (e.g., MoO₃, WO₃, etc.),^[48,49] or other compounds like K₂MoS₄^[58] can be applied during the synthesis process. The yield of fabrication by using CVD method is much higher than that of micromechanical exfoliation, and the quality

control is easier than that of liquid-based methods. However, due to the defect density inevitable during growth, the crystal quality is not as good as that by micromechanical exfoliation. In addition, the harsh growth conditions during CVD fabrication process, including high temperature and chemically active growth precursors, often limit the direct growth of 2D materials on specific substrates.^[50] Thereby, the follow-up steps that are used to transfer the 2D materials to arbitrary substrates is necessary.^[51,52] Whereas, the additional transfer steps are time-consuming and may introduce residues or defects which will deteriorate the material properties. On all accounts, synthesis of high-quality 2D material is essential for their optoelectronic applications, which needs continuous efforts in the near future.

As mentioned above, graphene was first obtained by micromechanical exfoliation as 2D materials.^[15] Graphene has attracted tremendous interest for optoelectronic applications due to its tunable interband transition, broadband light absorption ability (2.3% per layer), high thermal conductivity (5300 W m⁻¹ K⁻¹), and ultrahigh carrier mobility ($\approx 10^5$ cm² V⁻¹ s⁻¹).^[59–61] The available value of energy bandgap in intrinsic graphene is zero, which can be tuned from tens to hundreds of millielectronvolts through electrical gating,^[62] chemical doping,^[63–65] strain engineering,^[66,67] or in stacked-layer graphene^[68–70] and graphene nanoribbons (GNRs).^[71–73] Through pressure, trilayer graphene transforms from semimetal to semiconductor, obtaining a bandgap of 2.5 ± 0.3 eV.^[74] Recent advance in bottom-up synthesis of ultra-narrow GNRs make it possible to further tune the bandgap of graphene by changing the ribbon width and edge structure.^[75–79] The armchair GNRs with five carbons across the width synthesized on Au (111) surfaces is shown to have an unexpected large bandgap of 2.8 ± 0.1 eV.^[80] Nevertheless, for a practical implementation using GNRs, the influence of the line edge on the bandgap and the transport properties must be considered. It remains a great challenge to find ways of fabricating large size graphene with a sizable bandgap experimentally. These restrictions have led to the search for other 2D materials with sizable bandgap.

Beyond graphene, a multitude of 2D materials with various optoelectronic properties have been explored, including insulators (for instance, h-BN^[81,82]), semiconductors (for instance, TMDCs,^[83–85] BP,^[86–88] silicene and germanium,^[89,90] arsenene and antimonene,^[91,92] etc.), and superconductors (for instance, Mo₂C,^[93] atomically thin Ga,^[94] etc.). Their bandgaps vary from zero in superconductors to several electronvolts in insulators. The bandgap distributions of typical 2D materials are shown in **Figure 2**. Among them, h-BN has a graphite-like structure, a large electrical bandgap (≈ 5.5 eV), a high chemical stability, excellent mechanical properties, as well as good thermal conductivity.^[95,96] Layered h-BN is an appealing dielectric and electrically insulating substrate because it has an atomically smooth surface that is relatively free of dangling bonds and charge traps.^[97] TMDCs, such as MoS₂, MoSe₂, WS₂, and WSe₂, have moderate bandgaps (1–2 eV) that change from indirect in bulk to direct in monolayer.^[26] A sphere diameter engineering technique has been designed to tune the bandgap of TMDCs within a continuous range of 360 meV.^[98] These materials show many interesting properties, including thickness-dependent bandgaps, relatively high carrier mobilities, and high optical absorption coefficients, holding great potential for nanoelectronic and

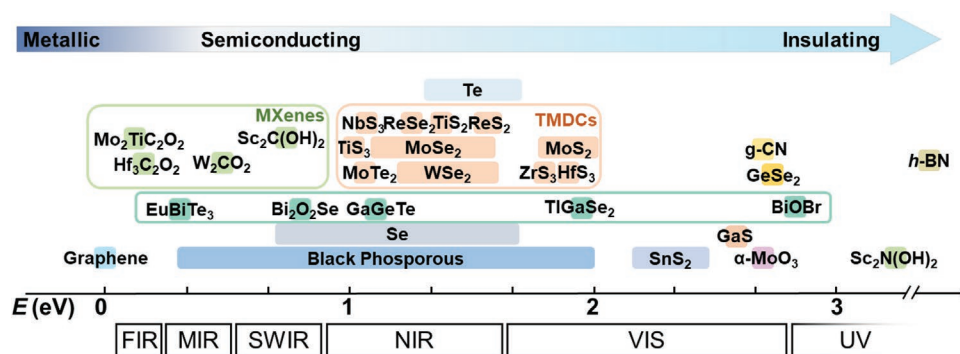


Figure 2. Bandgap distributions of typical 2D materials.

optoelectronic applications.^[99,100] BP is the most stable allotrope of the phosphorus element in standard conditions. This material has a tunable direct bandgap from bulk (0.3 eV) to monolayer (1.5–1.8 eV), which benefits the light–matter interactions in BP in infrared band.^[101] Along with its thickness-dependent bandgap, BP also displays high carrier mobility in the order of $10\,000\text{ cm}^2\text{ V}^{-1}\text{ s}^{-1}$ in bulk and $1000\text{ cm}^2\text{ V}^{-1}\text{ s}^{-1}$ in flakes, signifying that BP is a very promising 2D material for optoelectronic applications, especially in infrared band.^[19,102] On the other hand, monolayer arsenene and antimonene are predicted to be indirect semiconductors with bandgaps of 2.49 and 2.28 eV, posing potential for optoelectronic devices working in blue or ultraviolet (UV) range.^[103] More recently, 2D perovskites have received increasing attention mainly due to their tunability of optical and electronic properties through quantum-size effects (particularly when the thickness is lower than their exciton Bohr radius), sizeable bandgap (1.2–2.4 eV), strong optical absorption, low nonradiative recombination rate, long carrier diffusion length, and solution processability.^[104,105]

Furthermore, layered 2D materials with atomically uniform thicknesses can be stacked on top of each other, where adjacent layers are held together by van der Waals (vdW) forces in the stack with atomically sharp interfaces.^[106] Such vdW heterostructures can be composed of a variety of 2D materials in different combinations, thereby an unprecedented degree of control of their electronic and optical properties is achievable.^[28,107,108] Notably, vdW heterostructures also have tunable band alignment, lack of lattice mismatching, atomically steep carrier gradient, fast charge transport, strong light–excitons interactions, and magnetic properties, which can be used for electronic, optoelectronic, spintronic, valleytronic, and electromagnetic devices.^[109–111] The optoelectronic properties of vdW heterostructures can be tuned by gate voltage, strain, and its twisted angle.^[112,113] The diversity of 2D materials offers many possibilities to design advanced heterostructures. These properties differ the vdW heterostructures from traditional heterostructures, and bring about some novel physical phenomena.^[114] For instance, resonant tunneling can be realized by the proper alignment of two 2D layers.^[115,116] Moiré patterns are observed due to the enhanced electron orbitals coupling in the adjacent 2D materials.^[117,118] So far, 2D heterostructure have been used in optoelectronic applications including LEDs, photodetectors, photovoltaic devices, and so on.^[109,119,120] Notably, vdW heterostructures have atomically thin charge transport path, which

can be used to realize ultrafast switching speed in optoelectronic devices.^[121]

3. Light Sources Based on 2D Materials

In the optoelectronic circuits, the light source provides the energy and information for photonic devices handling. Thereby, light source is one of the vital components of integrated optoelectronics. However, it is difficult to realize on-chip light source in silicon based integrated optoelectronics. Common approaches for light sources are using one or few off-chip or wafer-bonded lasers based on III–V materials, which is limited to implement on-chip integration. Light sources with high efficiency, spectral tunability, and device integrability are of great significance for display, lighting, optical interconnect, and sensing applications. Specially, on-chip light source which allows high-density integration greatly exceed the off-chip light source in terms of energy efficiency and scalability. Low preparation cost and easy integration with silicon make 2D materials better candidate in the application of on-chip light source. In addition, tunability of the bandgaps of 2D materials implies that devices on based 2D materials can cover a tunable spectral range.

The lack of a bandgap in graphene makes the electron–hole recombination inefficient to emit light due to the rapid energy dissipation. But graphene can be used as thermal light emitter due to its superior thermal conductivity and high-temperature stability. Graphene heated by an electrical current can emit near-infrared light though the efficiency is extremely low.^[122] Bright visible light emission can be observed in the suspended graphene under an electrical bias, and the emission spectrum can be tuned by adjusting the distance between the graphene and substrate due to the strong optical interference between them.^[123] Figure 3a shows the schematic illustration of an electrically biased suspended graphene device. In this device, spatially localized hot electrons ($\approx 2800\text{ K}$) at the center of the graphene layer led to a 1000-fold enhancement in thermal radiation efficiency, providing an alternative way towards atomically thin, flexible, and transparent light emitters. An electrically driven graphene-based light emitter can generate pulses up to 10 GHz from visible to near-infrared.^[124]

TMDCs with appropriate bandgap are attractive materials for light emission. Like graphene, devices based on MoS_2 can

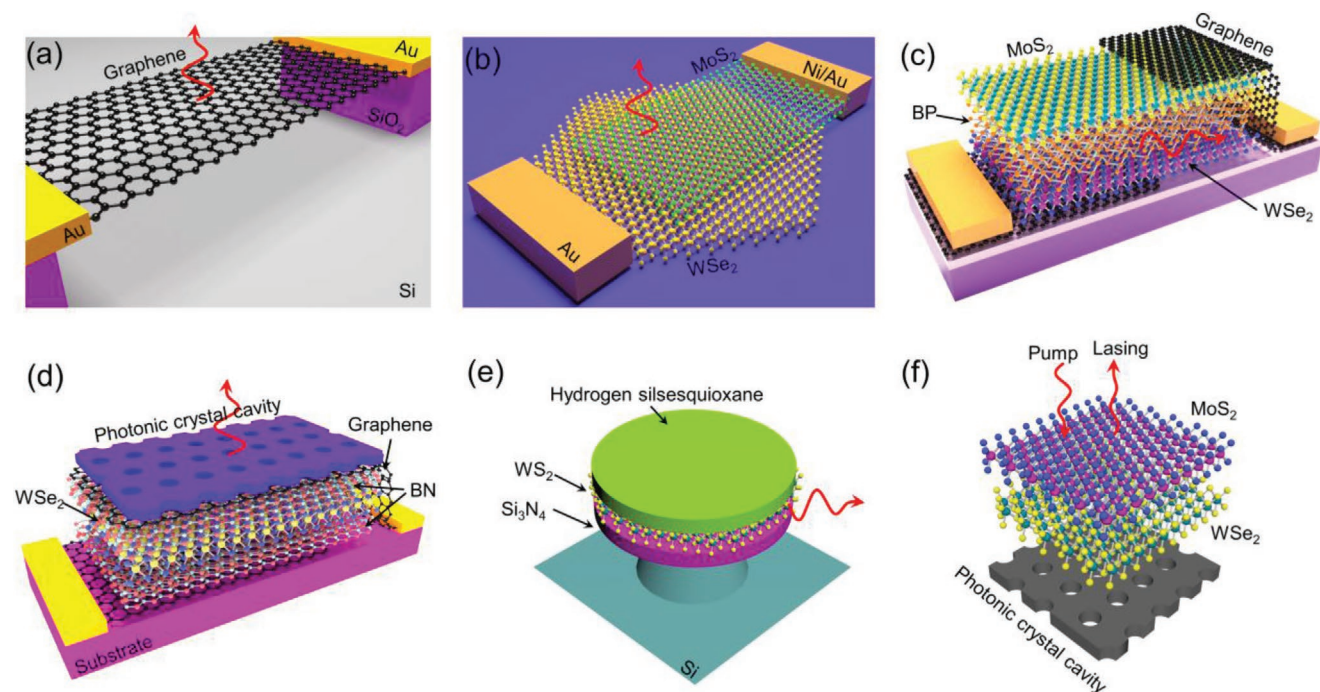


Figure 3. Light sources based on 2D materials. a) Schematic of electrically biased suspended graphene thermal emitter.^[123] b) Schematic of the WSe₂/MoS₂ vertical heterojunction LED.^[128] c) Schematic of an infrared LED that uses multiple layers of narrow-bandgap BP and larger-bandgap TMDCs.^[131] d) Schematic of a vdW heterostructures light emitting tunneling diodes integrated with a nanocavity.^[132] e) Schematic of an optical-pumped continuous-wave laser based on monolayer WSe₂ integrated with photonic crystal cavity.^[134] f) Schematic of an optical-pumped laser based on MoS₂/WSe₂ heterostructures on silicon photonic-crystal cavity.^[139]

also work in thermal light emission benefiting from its large Seebeck coefficient. A free-standing monolayer MoS₂ sheet can emit visible light as a result of Joule heating.^[125] TMDCs own large exciton binding energies which also bring them high exciton radiative rate. Electroluminescence of monolayer MoS₂ has been realized.^[126] Typically, an efficient LED requires the formation of a p-n junction, which facilitates the effective recombination of injected electrons and holes. Lateral p-n junctions in a TMDC layer can be realized by applying a sufficiently large bias to locally invert the potential of the TMDC channel with respect to the gate. A silicon waveguide-integrated LED based on bilayer MoTe₂ lateral p-n junction was realized, providing a new option for on-chip light sources.^[127] In addition to the lateral p-n junctions, the creation of vertical p-n junctions also leads to efficient light-emitting from TMDCs. Instead of selectively doping TMDCs into p-type or n-type semiconductors, Figure 3b shows an atomically thin and sharp heterojunction p-n diode by vertically stacking p-type monolayer WSe₂ and n-type MoS₂.^[128] The electroluminescence studies showed prominent band edge excitonic emission and strikingly enhanced hot-electron luminescence with distinct layer-number dependent emission characteristics due to electron-orbital interaction in TMDCs.

Recent reports also show that defects in 2D materials favor single photon emission. Electrically driven single photon emission from 2D TMDCs (e.g., WSe₂, WS₂) has been demonstrated by using vdW heterostructures. A single photon emitter based on the vertical heterojunction structure with the electrostatically defined graphene-h-BN-WSe₂ p-i-n junction was constructed.^[129] The light emission mainly relies on optical excitation of single

defects in isolated WSe₂ monolayers, while graphene is used as the electrodes and h-BN as the dielectric spacer layers. Similar to optically excited defect bound excitons, narrow spectral lines and a doublet in the electroluminescence spectrum were observed at low current densities and low temperatures (≈ 5 K), arising from spatially localized defect regions of the WSe₂. An electrically driven single photon-emitting device consisting of graphene, h-BN, WS₂ was also fabricated, showing the prospect of 2D materials as a new platform for single photon emitters.^[130] These findings are consistent with other single photon emitters based on electrically driven 2D TMDCs, together paving the way for on-chip and electrically driven single photon sources for quantum technology applications.

To boost the external quantum efficiency (EQE) of TMDCs based LEDs, 2D quantum well (QW) structure was developed by Novoselov and co-workers.^[109] A high EQE of $>8\%$ was achieved by band-structure engineering with one atomic layer precision. The creation of multiple QW heterostructures also allows fine-tuning of the emission spectra by combining 2D semiconductors of different bandgaps. The compatibility of these QW-based heterostructures was further verified on elastic and transparent substrates, promising to yield high quantum efficiency LEDs based on 2D materials. As an important member of 2D materials family, BP is also promising in constructing infrared LEDs. Figure 3c shows a potential LED using multiple layers of narrow-bandgap BP and larger-bandgap TMDCs.^[131] The BP, which has a tunable direct-bandgap by varying the layer numbers, can be used as an active semiconductor for light emission, while p-type WSe₂ and n-type MoS₂ can facilitate the

injection of holes and electrons, respectively. Therefore, the band-offset at the BP-TMDCs interface enables the recombination of injected carriers within BP for efficient light emission. A nanocavity integrated vdW heterostructures, comprising of graphene/h-BN as top and bottom tunneling contacts and monolayer WSe₂ as an active light emitter, was also fabricated as light-emitting tunneling diodes, as shown in Figure 3d.^[132] By integrating a photonic crystal nanocavity on top of the vdW heterostructure, the device emitted single-mode light with a high degree of linear polarization (84%), and the single mode emission can be modulated at a speed of \approx MHz, further proving that the vdW heterostructures hold great potential for on-chip optical information technologies. An enhanced light emission was also achieved through coupling of WSe₂ monolayers with circular Bragg grating structures, which suggests the potential for on-chip light sources by integrating monolayer TMDC and optical resonator.^[133]

In addition, large binding energy and the absence of dangling bonds make 2D materials, especially TMDCs, to be effective gain materials for generating lasers. An optical-pumped continuous-wave laser with ultralow thresholds was achieved by introducing monolayer WSe₂ as a gain medium which confines direct-gap excitons to surface of photonic crystal cavity (Figure 3e).^[134] The fabrication of the device shows the feasibility of using 2D materials as the gain medium to realize on-chip nanolasers. A MoS₂ lasers made by coating MoS₂ between SiO₂ microdisk and microsphere exhibited attractive performance like room-temperature operation, low threshold of 5 μ W, and large output power, facilitating the development of 2D materials based lasers on silicon.^[135] A vertical cavity surface-emitting laser, consisting of dielectric oxides as distributed Bragg reflectors and WS₂ as a gain medium, was reported operation at room temperature with a low threshold of 5 nW.^[136] Recently, silicon photonic-crystal cavity was combined with TMDCs to produce laser operation at room-temperature.^[137] A 1305 nm infrared laser based on few-layered MoTe₂ and silicon photonic-crystal cavity was achieved.^[138] Besides, vdW heterostructures can also generate lasers. Figure 3f demonstrates an optical-pumped laser based on MoS₂/WSe₂ heterostructures on silicon photonic-crystal cavity.^[139] The device works in infrared range with a threshold of 33 μ W, opening up a new prospect for the development of coherent light sources with customized optical properties on silicon photonic platforms.

Beyond TMDCs, perovskite-based LED was first reported in 2014, bringing breakthroughs to low-cost, solution-processible, high-performance LEDs.^[140] Perovskite LEDs exhibit high defect tolerance and high color purity. The light-emitting properties can be easily tuned via compositional and structural engineering of perovskite.^[141–143] The solution-processed perovskites with spontaneously formed sub-micrometer-scale structures can effectively extract light from the device and retain wavelength- and viewing-angle-independent electroluminescence, achieving peak external quantum efficiencies of 20.7%.^[144] Visible light emitting perovskite LED with over 20% quantum efficiency can be achieved using a CsPbBr₃/CH₃NH₃Br quasi-core/shell structure.^[145] The structure simultaneously provides high luminescence and balanced charge injection. In addition, perovskite is an important candidate for low-cost laser applications due to its high optical gain, balanced carrier mobility, and

low-temperature solution-processability. The optically pumped perovskite lasers have been developed. But the development of electrically pumped perovskite laser is still in its infancy. Furthermore, the stability of perovskites under electric stress and a large efficiency roll-off under high current injection level is the major obstacles to its further development.

4. Optical Modulation Based on 2D Materials

Optical modulation is one of the main required functionalities for integrated optical interconnects. An optical modulator is a device that can change one or few attributes of light, such as its intensity, amplitude, frequency, phase, or polarization. Depending on the change of material property that is used to modulate light, optical modulators can be categorized into absorptive modulators and refractive modulators. In the former ones, absorption coefficient of the material is changed, while in the latter ones, refractive index of the material is changed, which in turn changes the behavior of light propagation. A set of figures of merit are used to characterize an optical modulator, including modulation speed, modulation depth, bandwidth, insertion loss, footprint, and power consumption. Details on the definitions of modulator figures of merit can be found in ref. [14]. Optical modulators with fast modulation speed, high modulation depth, broad bandwidth, low insertion loss, small footprint, and low power consumption are preferred for optical interconnects in future integrated optoelectronic systems. In the past few decades, semiconductor optical modulators based on Si, GeSi, and III–IV semiconductor compounds have been intensively studied. However, they suffer from large footprint, non-compatibility with CMOS technology or narrow bandwidth. In contrast, graphene holds a great potential to be used for optical modulators owing to its tunable absorption property and refractive index by external disturbance (such as applying an electric field), compatibility with CMOS technology, and broad bandwidth.

Absorptive modulators with graphene have been demonstrated covering the visible,^[146,147] infrared,^[24,148] and THz range.^[149,150] Optical response of these devices at visible and near-infrared frequencies is dominated by interband transition of graphene, while dominated by intraband transition of graphene in far-infrared and THz frequencies.^[146] A typical graphene electro-optic modulator has been fabricated where graphene was placed adjacent to a silicon optical waveguide, as shown in Figure 4a.^[24] The silicon waveguide also acts as a back gate to electrically tune the Fermi level of the graphene sheet, thereby modulating its light absorption property through Pauli blocking. Optical absorption happens only when the Fermi level falls between the thresholds of $\pm\hbar\omega/2$ (\hbar is the reduced Planck constant, ω is the light angular frequency), otherwise graphene is quite transparent. Consequently, this modulation of optical absorption changes the intensity of light traveling through the silicon waveguide. The device shows good modulation performance, including a broad infrared operation spectrum (1.35–1.6 μ m), low operation voltage, and small footprint in the order of μ m², and a 3 dB modulation speed of 1.2 GHz. Optical modulators should feature low insertion loss for modern telecommunication links. The insertion loss

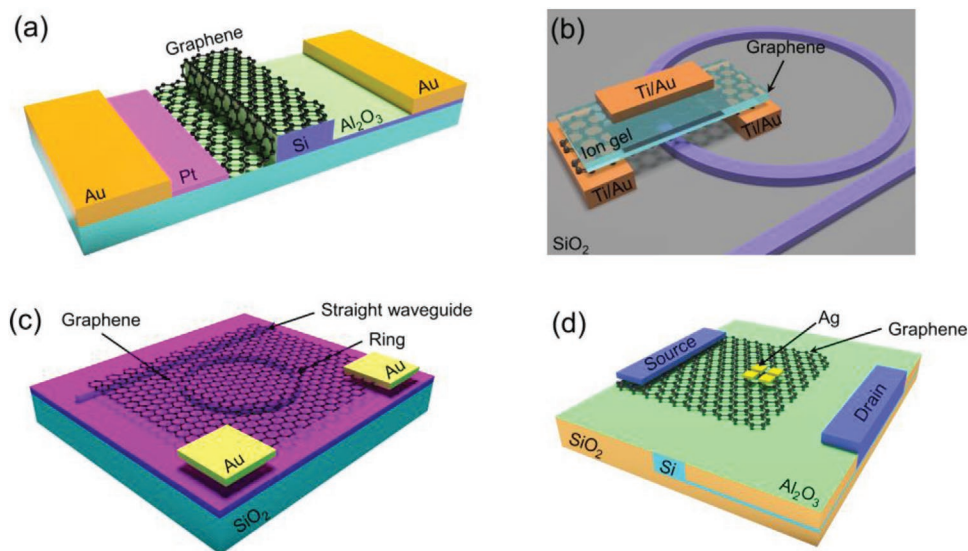


Figure 4. Optical modulators based on graphene. a) Schematic of a graphene-based waveguide-integrated optical modulator.^[24] b) Schematic of a graphene/ion-gel heterostructure incorporated with a silicon nitride microresonator for frequency modulation.^[154] c) Schematic of a thermo-optic modulator based on graphene.^[155] d) Schematic of an electro-optic modulator integrated with plasmonic patch array and graphene.^[160]

caused by graphene when the device is at “on” state is negligible as the intraband absorption of graphene is extremely low at near-infrared wavelengths. A graphene/graphene capacitor consisting of two sheets of monolayer graphene and an inter-layer dielectric is integrated to a segment of a silicon nitride ring resonator to realize effective electro-optic modulation.^[151] The device exhibits 30 GHz bandwidth. The speed of the device could be further improved by decreasing capacitor load, the graphene sheet resistance, and graphene/metal contact resistance. A graphene-sandwiched modulator was further proposed, in which two graphene layers are placed inside the silicon waveguide to increase the overlap between graphene and the optical mode.^[152] Graphene was placed at the location where maximum optical field occurs, separated the waveguide into two parts. The predicted bandwidth of this modulator is up to 55 GHz. However, this structure requires complicated processing and a very high standard of fabrication technology, thereby would be difficult to implement.

Another type of modulator is refractive modulator. A model of graphene-based ring resonator has been proposed in 2011.^[18] A minor variation of the effective refractive index in the ring resonator induced by the carrier plasma effect or the thermal effect, would shift the resonant peaks or change their intensities, consequently changing the behavior of light propagation in the device. By electrically tuning the Fermi level of graphene, both the quality factor and resonance wavelength of the silicon resonator were changed, which in turn modulate the amplitude of light in the silicon resonator. This kind of device configuration is supposed to deliver reduced dimension and high extinction ratio. Strong amplitude modulation $\approx 40\%$ at $1.55 \mu\text{m}$ wavelength was achieved in a graphene based modulator coupled with a silicon resonator.^[153] Furthermore, a graphene/ion-gel heterostructure was incorporated with a silicon nitride microresonator for frequency comb generation, as demonstrated in Figure 4b, where an ion-gel capacitor is implemented on top of the graphene.^[154] The graphene optical

group velocity dispersion can be gate-tuned from anomalous to normal dispersion and back to anomalous, rendering the possibility of frequency comb generation in the graphene-based microresonator. However, the modulation speed of this device is limited to hundreds of kilohertz because of the large ion-gel capacitance and slow ion diffusion. The speed may be further improved by adopting a high- κ gate dielectric.

It is noteworthy that the thermal conductivity of graphene is very high ($5300 \text{ W m}^{-1} \text{ K}^{-1}$), enabling efficient and fast heat transfer. Graphene can induce a fast temperature variation of about 100°C when 12 mW electrical power is applied. Figure 4c shows a thermo-optic modulator consisting of monolayer graphene on a silicon mirroring resonator.^[155] The effective refractive index of the mirroring can be efficiently tuned via graphene heating on top of it, thereby, the resonant wavelength and strength will be modified. The device demonstrated a modulation depth of 7 dB, operation power of 28 mW , and a small footprint of $10 \mu\text{m}^2$. Compared with the state-of-the-art silicon based thermo-optic ring modulators, the operation power and modulation depth fall almost on the same level, but the response speed is improved from typical microseconds to nanoseconds. It is expected that the proposed device has the potential for operation at tens of MHz by further reducing the resistance-contact constant.

For future optical data processing, a modulation rate larger than 100 GHz is needed. An all-optical approach is an optical solution to ultrafast signal processing beyond 100 GHz and the fiber-compatible scheme is one of the potential strategies for future on-chip optical interconnects.^[156] It was reported that graphene all-optical modulation can operate at a modulation bandwidth of 200 GHz .^[157] The bandwidth is limited only by the intrinsic graphene response time, since there is no need for electrical contact and circuitry drive. Surface plasmonic polariton (SPP) have also been exploited to realize ultracompact optical modulation with small footprint and fast modulation speed.^[158,159] A localized plasmonic enhanced

waveguide modulator, where silicon waveguide is integrated with plasmonic metal patch array and a layer of graphene, is reported as shown in Figure 4d.^[160] A voltage is applied to graphene in order to modify the resonance of the plasmonic metal patch. When the plasmons are tuned on- and off-resonance by the gated graphene sheet, a 400 GHz modulation rate can be achieved, which can meet the requirement of optical data processing. However, the loss associated with metal surface plasma is unacceptably large. The recent studies of vdW materials offer a new solution to achieve low-loss plasmons. For example, graphene SPPs have the potential to bypass major hurdles associated with plasmons in metals, such as the narrow spectral ranges and high optical losses, because graphene plasmons are electrically tunable and have a high degree of electromagnetic confinement.^[161,162] Investigating high-quality graphene based plasmonic waveguide may reveal low optical losses and other unanticipated optical properties, providing a basis for realizing low-loss plasma-assisted modulators.

Except for the graphene-based modulators, optical modulators using different kinds of 2D materials, such as TMDCs (WSe₂,^[163] WS₂,^[164] MoS₂^[165]), BP,^[166] and Te^[167] have been reported. A CVD-grown WSe₂ covered microfiber knot resonator (MKR) realized all-optical power modulation due to their resonance strong absorption.^[163] BP is also integrated to realize all-optical modulator due to the high carrier mobility, strong light-matter interactions and tunable bandgap.^[166] The modulator exhibited large bandwidth (3 dB bandwidth of ≈2.5 MHz) and a low-loss. In addition, 2D Te can be used for extremely fast and low energy Pockels effect modulators because of its broken structural inversion symmetry and giant electrooptic activity.^[167]

5. Photodetectors Based on 2D Materials and Their Hybrids

Photodetectors can convert incident light into a measurable photocurrent or photovoltage for further processing. Commercialized photodetectors based on IV and III-V semiconductor compounds (e.g., Si, Ge, GaAs, GaN, InGaAs) cannot respond to photons with energy lower than the material's bandgap. In contrast, graphene photodetectors are advantageous especially in terms of the spectral bandwidth. Its linear and gapless band structure ensures that its optical absorption coefficient is essentially constant from the visible to the MIR band.^[18] Because of this spectrally flat absorption, graphene photodetectors can convert light into electrical signal over a broad electromagnetic spectrum. A typical graphene photodetector with interdigital electrodes is shown in Figure 5a. Because of its ultrafast carrier mobility (up to 10⁵ cm² V⁻¹ s⁻¹) and fast exciton relaxation time (<150 fs), graphene photodetectors have shown ultrafast photoresponse with the operation frequency predicted to be ≈500 GHz.^[168] However, the performance of graphene photodetectors is strongly limited by the large dark current that dominates under nonzero bias operation. The responsivity of pure graphene-based photodetectors is limited to ≈10⁻² A W⁻¹, owing to its finite light absorption in such a thin body (one atomic layer thick) and ultrafast interband and intraband recombination rate of the photo-excited carriers.^[169,170] For comparison, the responsivity of commercial Si and Ge photodiodes lies in the range of 0.5–1 A W⁻¹. To bridge this gap, tremendous efforts have been devoted to enhance the light absorption in graphene, such as coupling graphene with plasmonic nanostructures,^[171,172] microcavity,^[173,174] as well as other gain materials (e.g., PbS quantum dots^[175]), as shown in Figure 5b,c.

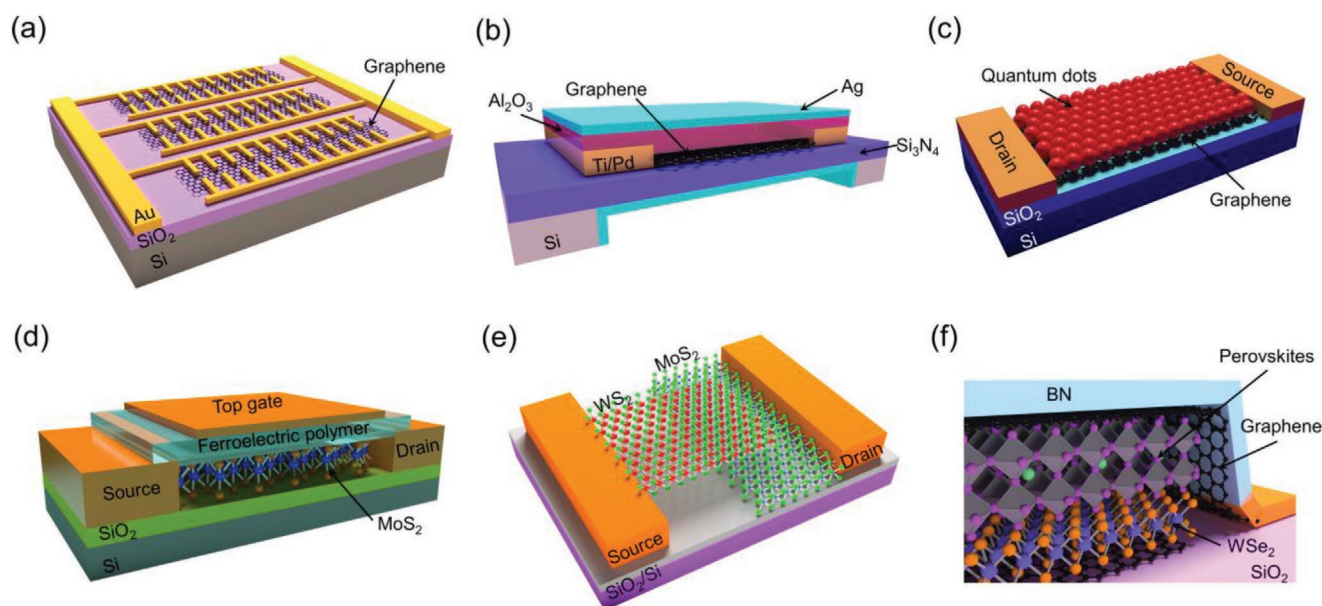


Figure 5. Representative photodetectors based on 2D materials. a) Schematic of a photodetector based on gold-patched graphene nanostrides.^[172] b) Schematic of a microcavity-integrated graphene photodetector.^[173] c) Schematic of a hybrid graphene-quantum dot photodetector.^[175] d) Schematic of a photodetector with ferroelectric polarization-induced electrostatic field.^[188] e) Schematic of a vertical heterojunction photodetector.^[231] f) Schematic of a vdW heterostructure photodetector made of multiple kinds of 2D materials.^[211]

TMDCs have also shown intriguing potential for photodetection, because Van Hove singularities in the electronic density of states of TMDCs guarantees enhanced light–matter interactions.^[176] As the most explored member from the family of TMDCs, MoS₂ has a tunable bandgap that varies with thickness, i.e., bulk MoS₂ has an indirect bandgap of 1.29 eV, and monolayer MoS₂ has a direct bandgap of 1.8 eV due to quantum confinement effect. Atomically thin films of MoS₂ have excellent photoactive properties in terms of strong resonant light absorption (>20%) which makes this material ideal for use in photodetectors.^[177–178] The responsivity of exfoliated monolayer MoS₂ can reach 880 A W⁻¹.^[179] Photodetectors based on multilayer MoS₂ films can achieve comparable responsivity and wider spectrum response than the monolayer MoS₂ photodetector due to the decreased bandgap of multilayer TMDCs.^[178] Apart from MoS₂, other TMDCs have also been explored for photodetection, including WS₂,^[180,181] WSe₂,^[182,183] MoSe₂,^[184,185] PtSe₂,^[23,186] etc. Alike the case for graphene photodetectors, the approaches used to improve the device performance is also applicable to TMDCs photodetectors. For instance, when incorporating graphene quantum dots (GQDs) onto MoS₂ to form an n-n type heterostructures, the device shows significantly improved photoresponsivity ≈10⁴ A W⁻¹ and a photogain ≈10⁷ electrons per photon.^[187] The improved photodetection performance is attributed to the enhanced light–matter interactions resulting from the tunneling of photoexcited carriers from the GQDs to MoS₂ and the reabsorption of emitted photons from the GQDs by MoS₂, which is different from the aforementioned ones in graphene/PbS hybrid structure,^[175] in which PbS QDs do not emit photons. However, the photodetection of MoS₂ photodetectors mainly lie in UV to visible wavelengths range induced by the relatively large bandgap (1–2 eV). The energy gap engineering of a 2D material system can be used to broaden this range. Under an ultrahigh ferroelectric polarization-induced electrostatic field (Figure 5d), the photoresponse wavelength range of a MoS₂ phototransistor was extended from the visible to the near-infrared range (0.85–1.55 μm).^[188] Additionally, the response speed of TMDCs based devices is relatively slower than that of graphene, on the timescale of milliseconds, due to the much smaller carrier mobility of TMDCs, and the relative long relaxation of the photocarriers in TMDCs.

BP has also emerged as an attractive candidate for optoelectronic applications.^[189] The bandgap of BP fits well into the gap between zero bandgap graphene and large bandgap TMDCs. BP photodetectors exhibit good photoresponse in a broad spectral range from visible to MIR wavelengths, and can also acquire high-contrast images both in the visible and infrared waveband, signifying that BP is a very promising 2D material for infrared photodetection.^[190,191] Additionally, BP has intrinsic in-plane electric and optical anisotropy.^[192] The hexagonally distributed phosphorus atoms in BP are arranged in a puckered structure. Due to this property, BP photodetectors are polarization sensitive.^[193,194] Higher photocurrents are generally found in the armchair direction than that in the zigzag direction because the interband transitions for polarization along the armchair direction are predominant over the zigzag direction, which thereby allows determination of the crystalline orientation. Other in-plane anisotropic 2D materials, for instance, As_{0.83}P_{0.17},^[195] GaSe,^[196] GeAs,^[197] PdSe₂,^[198] GeP,^[199] ReS₂,^[200]

ReSe₂,^[201] TiS₃,^[202] TiSe,^[203] Te,^[204] TaIrTe₄,^[205] MoTe₂,^[206] WTe₂,^[207] etc., also demonstrate polarization sensitive photoresponse. Recent report showed that an anisotropic Te photodetector with photoresponsivity anisotropic ratio reaching up to ≈8 under 2.3 μm illumination can realize polarized infrared imaging under scattering.^[208]

The successful production of 2D organo-metal halide perovskite promises novel device applications due to their high surface-to-volume ratio, sizeable bandgap, and high sensitivity to visible light. Organo-metal halide perovskite are materials described by AMX₃ formula, in which A is organic cation, M is metal cation, and X is halogen anion. Different halogen anions in perovskite materials affect optical bandgap which determine response spectra of photodetectors.^[209] Photodetectors based on single-unit-cell thick CH₃NH₃PbI₃ perovskite nanosheet shows a responsivity of 22 A W⁻¹ under a 405 nm laser, relative fast rise (20 ms) and delay (40 ms) times due to the reduced dimensionality.^[210] The 2D perovskite sandwiching between two graphene layers is used to enhance the device performance.^[211] Owing to the high mobility of graphene layers, the charge carriers would transmit very fast which in turn results in a high responsivity of 950 A W⁻¹. However, stability in ambient condition is still a major concern when considering the use of 2D organo-metal halide perovskite based photodetectors. Alternatively, 2D all inorganic perovskites (such as CsPbX₃, X is halogen anion), which show comparable performance in terms of light absorption to that of the organo-metal halide perovskites, seem to be potential candidates for stable and efficient photodetection.^[212] A photodetector based on atomically thin CsPbBr₃ nanosheets, demonstrated reasonable responsibility, high stability as well as outstanding flexibility.^[213] The simple solution processability of large-area, crack-free, high-quality 2D perovskites films makes it potential candidates for the fabrication of large area, ultrathin, and flexible optoelectronics. Other emerging 2D materials, including MXenes (Mo₂C^[214] MoCT_x,^[215] Ti₃C₂T_x^[216]), multielement 2D layered material (Bi₂O₂Se,^[217] EuSbTe₃^[218]), 2D Se^[219] and its composites (MoSe,^[220] GaSe,^[221] SnSe,^[222] PdSe₂,^[22] GaSe,^[223] Ga_{0.84}In_{0.16}Se^[224]), and 2D Bi^[225] have also been explored for photodetection with intriguing device performance.

Beyond above, vdW heterostructures include but not limited to graphene-h-BN, graphene-TMDCs, TMDC-TMDC combinations, have been intensively investigated for photodetection. A typical 2D heterostructure based photodetector is shown in Figure 5e. Heterostructures can combine the merits of different 2D materials, enabling good performance of the devices. The built-in electric field in the heterostructures accelerates the separation of photoexcited carriers, yielding a large photocurrent and a high quantum efficiency. Moreover, novel physical and optical properties inside vdW heterostructures may be achieved due to strong layer-layer coupling.^[226] The combinations of MoS₂/WSe₂,^[227,228] MoS₂/WS₂,^[229] WSe₂/ReS₂,^[230] etc., have been used in fabricating high-performance photodetectors. The I–V characteristics of these heterostructures behave prominent rectification effect, like the cases of traditional p-n diodes. Notable, the polarity of the photocurrent can be altered, and is quantitatively explained by the gate-tunable charge exchange between the heterostructure layers. Large-scale, periodic array of vdW heterojunctions can be produced recently.^[231–233]

Photodetectors using the heterojunction arrays were also demonstrated with reasonable performance. Additionally, as shown in Figure 5f, vdW heterostructures made of multiple kinds of 2D materials can also be explored for photodetection, demonstrating gate-tunable photodiode behavior.^[211] In the future, 2D vdW heterostructures promise to accomplish high performance optoelectronic devices which have fast operation speed, high absorption cross-section and small feature size. In **Table 1** of this part, we summarize the device figures-of-merit of photodetectors based on different 2D materials.

6. Electronic Circuits Based on 2D Materials

Electronic circuit is one of the indispensable parts in optoelectronic integration. FET is the basic unit cell of electronic circuits, as the functions of switch, amplifier, and so on. The development of FETs promotes the development of integrated optoelectronic circuits to a certain extent. 2D semiconductors are ideal candidates for FETs application which is expected to hold several merits including switchable conductance at atomic scale, high carrier mobility, free of surface dangling bond, and

Table 1. Comparison of device performances of photodetectors based on different 2D materials.

	Thickness	V_g, V_d [V]	Spectral range [nm]	EQE [%]	Responsivity [$A W^{-1}$]	Gain	Detectivity [$cm Hz^{1/2} W^{-1}$]	Response speed/rise time	Ref.
G ^{a)}	1 layer	-15, 0.4	1550	0.1–0.2	6.1×10^{-3}	–	–	16 GHz, 10 Gbit s ⁻¹	[234]
G/Au	1 layer	0, 0	514	1.5	6.1×10^{-3}	–	–	532 kHz	[235]
G/Microcavity	1 layer	0, 2	864.5	–	21×10^{-3}	–	–	–	[236]
G/PbS	1 layer	-20, 5	600 532, 950, 1450	25	$\approx 10^7$ (@600 nm)	$\approx 10^8$	7×10^{13}	10 ms	[175]
G/Perovskite	1 layer	0, 3	250–700	–	6.0×10^5 (@405 nm)	10^9	–	120 ms	[237]
MoS ₂	1 layer	50, 1	400–670	–	7.5×10^{-3} (@550 nm)	–	–	50 ms	[238]
MoS ₂	Trilayer	0, 10	<660	10	0.57 (@532nm)	13.3	10^{10}	70 μ s	[239]
MoS ₂	30 nm	-3, 1	UV=900	–	0.1 (@633 nm)	–	3×10^{10}	–	[240]
MoS ₂	1 layer	-70, 8	400–680	–	880 (@561 nm)	–	–	4 s	[179]
MoS ₂	Trilayer	0, 5	Vis ^{b)} = 1550	–	2570 (@635 nm)	–	2.2×10^{12}	1.8 ms	[188]
MoS ₂ /GQD	Trilayer	80, 1	<635	–	10^4 (@405 nm)	10^7	–	70 ms	[187]
WS ₂	60 nm	0, 9	370–1064	101	0.51 (@635 nm)	–	1.93×10^9	4.1 s	[241]
MoSe ₂	1 layer	0, 10	532	–	13×10^{-3}	–	–	60 ms	[242]
MoSe ₂	1 layer	0, 1	650	–	–	5×10^{-4}	–	<25 ms	[184]
BP	3–8 nm	0, 0.2	Vis = 940	–	4.8×10^{-3} (@640 nm)	–	–	1 ms	[19]
BP	120 nm	0, 0	Vis–NIR ^{c)}	–	20×10^{-3} (@532 nm) 5×10^{-3} (@1550 nm)	–	–	≈ 0.25 ms	[191]
Perovskite	1 unit cell	0, 1	405 532	–	22 (@453 nm) 12 (@532 nm)	–	–	<20 ms	[105]
G/Waveguide	1 layer	0, -1.5	NIR–MIR	–	0.13 (@2750 nm)	–	–	–	[243]
G/Waveguide	Bilayer	0, 1	1450–1590	<3.8	0.108	–	–	20 GHz 12 Gbits ⁻¹	[244]
G/Waveguide	Trilayer	0, 0	1310–1630	<10	0.05 (@1550 nm)	–	–	18 GHz	[245]
BP/Waveguide	11.5 nm	-0.4, -8	1550	<10	0.135	–	–	2.8 GHz 3 Gbit s ⁻¹	[246]
MoS ₂ /WS ₂	Multilayer	0, 1	633	278	1.42 (@633 nm)	–	–	Thousands of seconds	[229]
G/MoS ₂	1 layer/5 layer	-50, 0.1	635	≈ 32	5×10^8	5×10^{10} 10×10^{10}	–	–	[247]
G/MoS ₂ /G	1 layer/ 50 nm/1 layer	-60, 0	458–633	27 (@514 nm)	–	–	–	50 μ s	[248]
G/MoS ₂ /Metal	1 layer/50 nm	-1, 0	458–633	55 (@488 nm)	0.22 (@488 nm)	–	–	–	[248]
G/WSe ₂		0, 1	532	800	0.35	–	10^{13}	50 μ s	[249]
G/Perovskite/G	1 layer/ 95–150 nm/layer	0, 1	532	–	950	2200	–	22 ms	[211]

^{a)}G: graphene; ^{b)}Vis: visible; ^{c)}NIR: near-infrared.

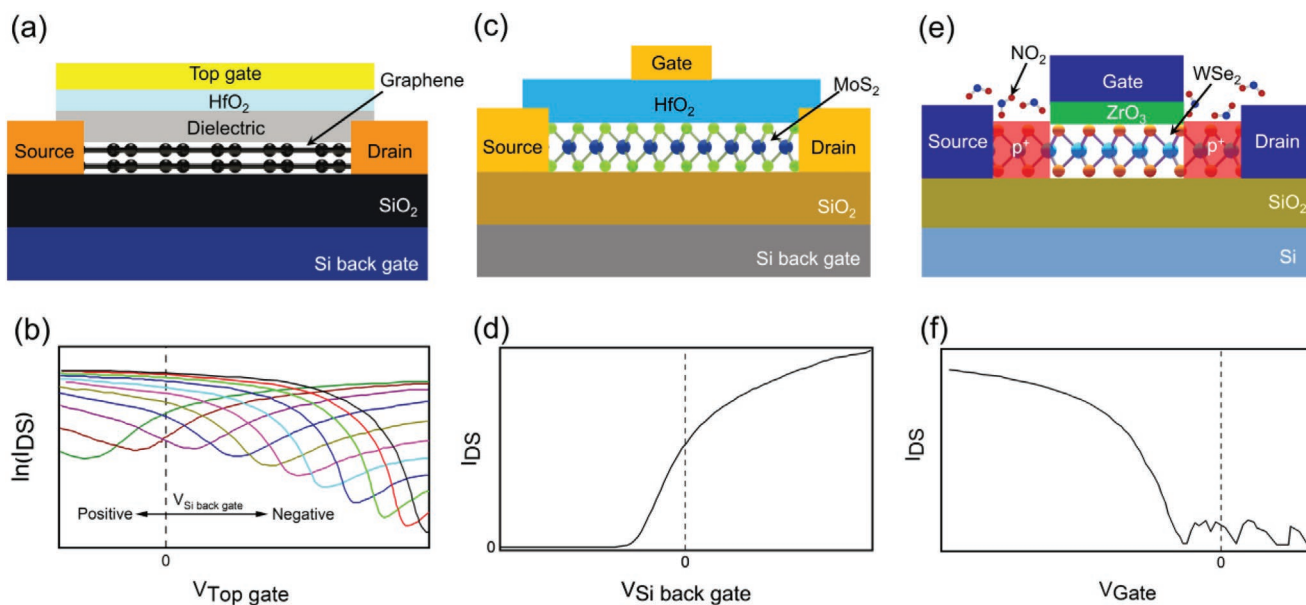


Figure 6. Characterization of FETs based on 2D materials: a) Cross sectional view of a dual-gate bilayer graphene FET.^[69] b) The room temperature transfer characteristics of a dual-gate bilayer graphene FET.^[69] c) Cross-sectional view of a dual-gate monolayer MoS₂ FET.^[258] d) Typical transfer characteristic for n-type MoS₂ FET.^[258] e) Schematic of a top-gate WSe₂ FET with chemically p-doped metal contacts by NO₂ exposure. Here, the top-gate acts as the mask for protecting the active channel from NO₂ doping.^[250] f) Typical transfer characteristics of a p-type WSe₂ FET.^[250]

compatibility with the current CMOS technology. In particular, their 2D feature, as the most significant advantage, enables the entire thickness of the active channel in close proximity to the gate electrode, thereby enhancing the gate control of the channel and reducing short-channel effect.

Graphene FETs offer advantages as they show extremely high mobility, high operation frequency, and good transparency. A graphene FET is demonstrated in **Figure 6a,b**. The graphene FET shows gate-tunable operation mode changing from n- to p-type mode as sweeping the gate voltages.^[69] However, in the context of electronic applications, the energy bandgap is one of the pivotal properties. An obstacle to use graphene has been the low on/off ratios (typically lower than 10²), resulting from the absence of an energy gap between its conduction and valence band. Such low on/off ratios are considered insufficient for digital electronic applications, which require at least four orders of magnitude current on/off ratios. Semiconducting TMDCs FETs offer many benefits including high on/off ratios, steep subthreshold swing, reduced short-channel effect, smaller dielectric constant than silicon, intrinsically low density of surface traps, and correspondingly low threshold voltage. The reported magnitude of the carrier mobility in TMDCs FETs ranges from 10 to around 700 cm² V⁻¹ s⁻¹, the on/off ratios are typically from 10⁶ to 10⁸. Notably, small subthreshold swing of 60 mV dec⁻¹ is achievable in 2D TMDCs FETs, which outperforms silicon metal-oxide-semiconductor FETs (*MOSFETs).^[250] A MoS₂ FET with sub-10 nm channel length was demonstrated, which exhibits high on/off current ratio (~10⁶–10⁷) and no obvious short-channel effects.^[251–256] A 2D transistor with a 1 nm physical gate was constructed with a MoS₂ bilayer channel and a single-walled carbon nanotube as the gate electrode, signifying the potential of TMDCs to solve the problems of silicon transistors scaling in the future.^[257]

The demonstration of n- and p-type transistors on the same substrate is needed to enable low-power logic circuits. Notably, TMDCs FETs can operate in n- or p-type mode, as seen in **Figure 6c–f**. Monolayer and few-layered MoS₂ has shown the potential use for high performance n-FETs, due to their low conduction band edge position and Fermi level pinning near the conduction band edge at the metal-TMDCs interfaces. Single-layer MoS₂ FET was reported to exhibit a high current on/off ratio of 10⁸ at room temperature, an electron mobility of over 200 cm² V⁻¹ s⁻¹.^[258] The reported values of on/off ratio and achievable mobility in a double layer MoS₂ FET are 10⁶ and 300 cm² V⁻¹ s⁻¹, respectively.^[259] The field-effect mobility of a 10-nm thick multilayer MoS₂ FET was reported to be 184 cm² V⁻¹ s⁻¹.^[260] MoS₂ FET built from all 2D materials, using a MoS₂ channel, h-BN gate dielectric, and graphene source/drain and gate contacts, demonstrates an on/off current ratio of >10⁶ and an electron mobility of ≈33 cm² V⁻¹ s⁻¹.^[261] On the other hand, WSe₂ and MoSe₂ are generally used for the exploration of high performance p-FETs, due to their high valence band edge position. Monolayer WSe₂ FET was reported with a high effective hole mobility of 250 cm² V⁻¹ s⁻¹, a subthreshold swing of 60 mV dec⁻¹, and on/off ratio of >10⁶ at room temperature.^[250]

Integrated circuit based on 2D materials has been reported with two n-type MoS₂ FETs, this configuration shows higher power dissipation than for circuits based on MOSFETs.^[262] Interestingly, in a single 2D material based Schottky-type FETs, the device transport polarity depends on the Schottky barrier height for electrons and holes, respectively.^[263] Layered WS₂ and WSe₂ are found to display ambipolar behavior, and this ambipolar operation is rarely observed in traditional FETs. By leveraging on the ambipolar transport behavior of TMDCs, complementary logic inverter can be realized. The operation

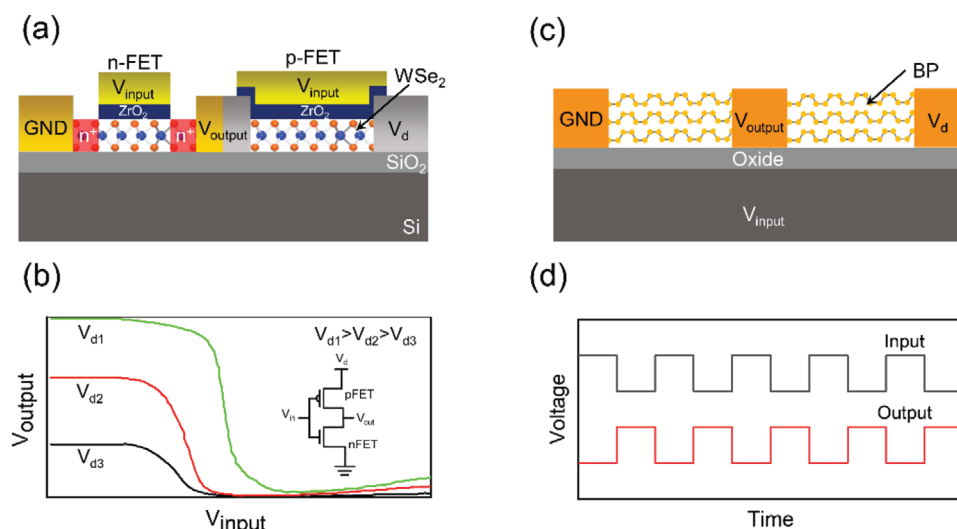


Figure 7. Characterization of FETs based on 2D materials. a) Schematic of an inverter based on WSe₂ complementary FETs, depicting the n- and p-FET components.^[264] b) Voltage transfer characteristics of a WSe₂ inverter at different supply voltages.^[264] c) Schematic of an ambipolar digital inverter based on BP transistor.^[267] d) Input pulse oscillates and output pulse of the inverter.^[267]

of n- and p-type FETs on the same WSe₂ flake was realized, and a complementary logic inverter has been demonstrated (Figure 7a,b).^[264] The peak direct current voltage gain is measured to be >12 and the noise margin for high input was 1.05 V at a small bias voltage of 3.0 V. Alike WSe₂, BP also demonstrates ambipolar conduction.^[265,266] A complementary inverter based on ambipolar BP FETs has been realized (Figure 7c,d).^[267] BP shows much higher carrier mobility of $\approx 1000 \text{ cm}^2 \text{ V}^{-1} \text{ s}^{-1}$ for the hole transport than that of TMDCs, allowing BP FETs to reach high-frequency operation up to 20 GHz.^[268] A carbon-doped BP (b-PC) FET achieved a higher p-type mobility of over $1995 \text{ cm}^2 \text{ V}^{-1} \text{ s}^{-1}$.^[269] A flexible BP FET has shown a device mobility of $\approx 310 \text{ cm}^2 \text{ V}^{-1} \text{ s}^{-1}$ and field-effect current modulation exceeding 10^3 .^[267] Based on this, flexible BP inverters, frequency doublers, analog amplifiers, and amplitude-modulated demodulators have been demonstrated. Following this, the radio frequency BP FETs on highly bendable polyimide substrate was reported for GHz nanoelectronic applications.^[270] The above results indicate that BP holds an important metric for high-speed electronics.

Table 2 summarizes typical device performances of FETs based on different 2D materials. For further application, several scenarios in the emerging 2D electronic circuits have to be carefully considered including interface traps, contact resistances, and device passivation. Though 2D semiconductors are deemed to be free of surface defects, a small but nonzero threshold voltage for 2D FETs is evidence of intrinsically low density of surface traps. A better 2D semiconductor/dielectric interface can be achieved if substituting the currently used SiO₂ with a state-of-art high- κ dielectric or h-BN. The second issue is the contact resistance at the TMDCs/metal junction, which is much larger than contacts of graphene/metal due to the enlarged Schottky barrier height induced by the wide bandgaps of TMDCs. Lowering the metal contact resistance is essential to harvest the intrinsic material properties, thereby it is important to choose contact metals with suitable work function.^[250,260,271] Lower work function metals like Sc are prior

to form improved contacts with n-type TMDCs,^[260] whereas higher work function metals like Pd are easier to form good contacts with p-type TMDCs.^[250] The third issue is isolating the 2D semiconductor from atmosphere because they are much more sensitive to introduced contaminants due to their ultrathin body thickness. Transistors passivated by a 20-nm-thick HfO₂ layer demonstrated a dramatic improvement in the field-effect mobility from 10 to $15 \text{ cm}^2 \text{ V}^{-1} \text{ s}^{-1}$ (before depositing HfO₂) to exceeding $300 \text{ cm}^2 \text{ V}^{-1} \text{ s}^{-1}$ (after passivation).^[259] Moreover, a significant enhancement in the field-effect mobility from 184 to $700 \text{ cm}^2 \text{ V}^{-1} \text{ s}^{-1}$ was achieved by covering the top of a MoS₂ transistor with a thin layer of 15-nm-thick Al₂O₃.^[260]

7. Nonlinear Photonics Based on 2D Materials

Nonlinear optics, which is a branch of optics investigating the light behavior in nonlinear media, plays an increasingly important role in optoelectronic applications. According to the fundamentals of nonlinear optics, the response of materials may cease to be linear under certain high optical field, and nonlinear optical effects could occur, where the higher-order ($n \geq 2$) terms appear at frequencies different from the frequency of the incident light.^[277,278] Compared with traditional bulk III–IV materials, 2D materials have comparable nonlinear susceptibility, ultrafast response, broadband and tunable optical absorption, and can be integrated to arbitrary substrates via vdW force avoiding the lattice-matching issue.^[279–282] Thus, the ease of integration and hybridization with other materials makes 2D materials a potential nonlinear optical platform for integrated nonlinear devices. The second-order nonlinear effects and third-order nonlinear effects are the mostly investigated processes recently. To date, the integration of these effects with integrated photonics is highly attractive for optoelectronic applications such as photon generation, manipulation, detection, imaging, and so on.^[283–286]

Table 2. Typical device performances of FETs based on different 2D materials.

	Thickness [nm]	Device structure	Polarity	Mobility [$\text{cm}^2 \text{V}^{-1} \text{s}^{-1}$]	On/off ratio [at 300 K]	Subthresh-old swing [mV dec^{-1}]	Output current [$\mu\text{A } \mu\text{m}^{-1}$]	Ref.
Graphene	1 layer	Bottom-gate	p-type	10^4	<30	–	$>10^8 \text{ A cm}^{-2}$	[15]
Graphene	Bilayer	Dual-gate	p-type	–	100	–	–	[69]
Graphene	1 layer	Top-gate	p-type	10^4	<5	–	–	[272]
CNRs	1.5	Bottom-gate	p-type	100–200	10^7	–	200	[273]
MoS ₂	1 layer	Top-gate	n-type	200	10^8	74	2.5	[258]
MoS ₂	15	Dual-gate	n-type	517	10^8	140	6.4	[274]
MoS ₂	Bilayer	Top-gate	n-type	300	10^7	88	23	[259]
MoS ₂	10	Bottom-gate	n-type	700	10^7	–	240	[260]
MoS ₂	10	Bottom-gate	n-type	33	$>10^7$	–	–	[261]
WSe ₂	1 layer	Top-gate	p-type	250	10^6	60	10	[250]
MoSe ₂	7	Bottom-gate	Ambipolar	150–200	10^6	–	1	[263]
WSe ₂	10	Top-gate	Ambipolar	–	$>10^4$	–	0.1–0.2	[264]
WSe ₂	8	Bottom-gate	p-type	350	10^6	250	–	[275]
BP	10	Bottom-gate	p-type	$1000(\mu_p^a)$	10^5	3700–13 300	≈ 1	[102]
BP	1 layer	bottom-gate	p-type	$286(\mu_p)$	10^4	–	194	[276]
BP	18.7	Bottom-gate	Ambipolar	$170.5(\mu_p)$	10^2	–	93.3	[265]
BP	15	Bottom-gate	Ambipolar	$310(\mu_p)$ $89(\mu_e^b)$	10^3 – 10^4	–	–	[267]

^{a)} μ_p : hole mobility; ^{b)} μ_e : electron mobility.

As to the second-order nonlinear effects, the second harmonic generation (SHG) in 2D materials is one of the mostly studied nonlinear process for integrated optoelectronic applications.^[279,280] The second-order optical effects are allowed due to their broken inversion symmetry in odd number of layers of TMDCs crystals such as MoS₂, MoSe₂, MoTe₂, WS₂, WSe₂, TiS₂, etc.^[287–293] The SHG in monolayer MoS₂ is orders of magnitude larger than that of bulk MoS₂.^[289] A monolayer MoS₂ was proved with strong optical nonlinear effects,^[287] and the second harmonic can be generated with a nonlinear susceptibility on the order of 10^{-7} mV^{-1} . The wavelength dependence of the SHG in monolayer MoS₂ was demonstrated with tunable excitation wavelengths from 680 to 1080 nm.^[288] Alike MoS₂, monolayer WS₂ also has large second order nonlinear susceptibility with an estimated value of $\approx 4.5 \times 10^{-9} \text{ mV}^{-1}$ which is nearly three orders of magnitude larger than other common nonlinear crystals such as BBO.^[291] In monolayer MoSe₂, the second-order susceptibility was calculated to be $\approx 5 \times 10^{-8} \text{ mV}^{-1}$ at the second harmonic wavelength $\approx 810 \text{ nm}$.^[292] Furthermore, the MoSe₂ monolayer exhibits a strong laser-induced damage threshold under picosecond-pulse excitation, which means MoSe₂ will be a promising candidate for high-power, thin-film-based nonlinear optical applications.

For optoelectronic applications based on SHG in 2D materials, a monolayer WSe₂ FET was demonstrated by electrical controlling of SHG intensity.^[293] The tunable SHG arises from the resonant responses of neutral and charged excitons under electrostatically controlled charging effects, which represent a new class of electrically tunable nonlinear optical devices. These CMOS compatible SHG transistors (**Figure 8a**) may enable novel applications in optical signal processing, on-chip

nonlinear optical sources, and integrated photonic circuits. By integration with waveguide, the length of the nonlinear interaction with light could be increased, and thus overcome the limitation of the monolayer thickness of TMDCs. As shown in **Figure 8b**, an atomically thin MoSe₂/Si-waveguide integrated platform was developed and demonstrated fivefold enhancement of the SHG in comparison to free-space SHG in bare MoSe₂.^[294] Integrating 2D crystals with microcavity can also achieve enhanced nonlinear output. A monolayer WSe₂ integrated with a planar silicon photonic crystal was reported for the improvement of SHG.^[295] By incorporating with the silicon photonic crystal, which has a high quality factor and small volume, the enhanced SHG (≈ 200 -fold enhancement compared to a bare monolayer on silicon) was observed when the excitation wavelength matched the cavity resonance wavelength. Furthermore, the enhancement of SHG by coupling a monolayer MoS₂ to the guided-mode resonances of a one-dimensional photonic crystal was demonstrated, and showing a 170-fold enhancement of the generated signal relative to a bare monolayer. This provides a way toward silicon chip-integrated nonlinear devices based on 2D materials.^[290]

As to the third-order nonlinear effects, the third-harmonic generation (THG) and four-wave mixing (FWM) are the mostly studied process in integrated optoelectronic applications.^[279,280] In contrast to SHG, THG can be possibly generated in materials regardless of whether they are inversion symmetry or not. The third-order nonlinear optical interactions in graphene have been extensively studied in experiments.^[296–298] Graphene has ultrafast nonlinear optics responses and displays a large third-order nonlinearity. A graphene layer integrated with a designed resonant cavity for THG was demonstrated

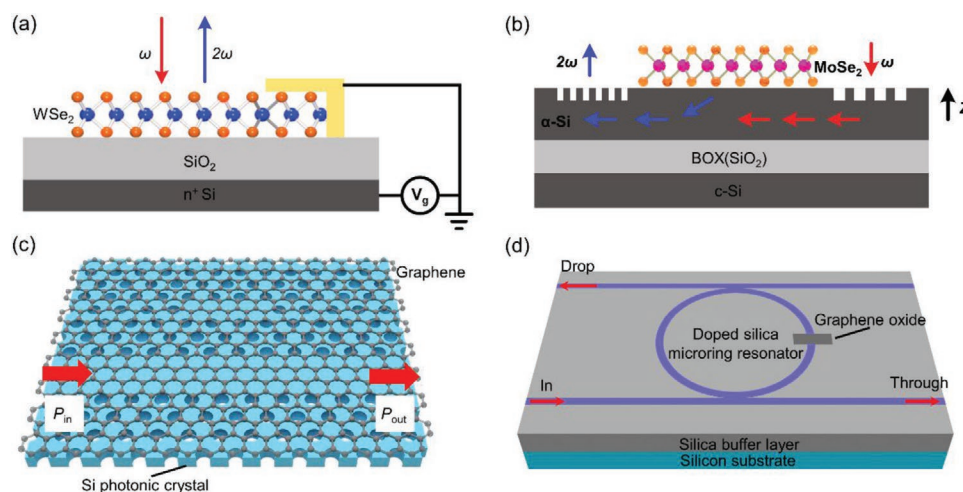


Figure 8. Nonlinear photonics based on 2D materials. a) Schematic of a monolayer WSe₂ transistor for SHG.^[293] b) Schematic of the hybrid integration of MoSe₂ onto a Si-waveguide for SHG.^[294] c) Schematic of the graphene integrated photonic crystal cavity for FWM.^[305] d) Schematic of graphene oxide films integrated with micro-ring resonators for FWM.^[306]

and the conversion efficiency approached 10^{-4} .^[299] Compared with the signal at nonresonant wavelength, a 117-fold enhancement of THG signal at resonant wavelengths was achieved from graphene integrated with the resonant cavity. The value of third-order susceptibility of graphene is deduced to be $4 \times 10^{-17} \text{ m}^2 \text{ V}^{-2}$. TMDCs including MoS₂, MoSe₂, WSe₂, WS₂, and ReS₂ have also demonstrated THG effects.^[300–302] In monolayer MoS₂, the third harmonic was reported to be around 30 times stronger than the second harmonic, and the THG efficiency for monolayer MoS₂ can reach three times higher than that of graphene.^[300] Interestingly, in ReS₂, the anisotropic THG was observed and the third-order susceptibility is on the order of $10^{-18} \text{ m}^2 \text{ V}^{-2}$.^[302] This large nonlinear optical response suggests potential applications of this material in optoelectronic devices involving third-order nonlinear processes.

FWM is one of a third-order nonlinear optical effects, in which light beams with different wavelengths interact with each other and produce new wavelengths.^[279,282] FWM in 2D materials is also employed for optoelectronic applications. In graphene and MoS₂ thin films, FWM was obtained by introducing pump probe laser beams with different wavelengths.^[303,304] As shown in Figure 8c, a graphene integrated with a wavelength-scale localized photonic crystal cavity was demonstrated for the high third-order nonlinear response.^[305] The chip-scale optoelectronic platform shows the exceptional third-order nonlinearity with ultralow-power optical bistable switching, self-induced regenerative oscillations, and enhanced coherent FWM at femtojoule cavity energies. The conversion efficiencies were observed up to 10^{-3} at a cavity Q-value of 7500 with low pump power of 600 μW . Layered 2D graphene oxide (GO) films integrated with CMOS-compatible doped silica micro-ring resonators (MRRs), as shown in Figure 8d, was also demonstrated for FWM generation.^[306] Due to the strong light–matter interactions between MRRs and GO film, a significant improvement was achieved in the FWM conversion efficiency for an MRR uniformly coated with one layer of GO and a patterned device with 50 layers of GO, respectively. Based on the above investigations, the integration of photonic resonators with 2D materials

has been proved to be an effective way to improve the performance of nonlinear optical processes.

8. Integration in Planar Silicon Photonics Based on 2D Materials

Layered 2D materials are well suited for integration in planar silicon photonics, because of their ultrathin body and compatibility with the current CMOS technology. The monolithic integration of a CMOS integrated circuit with graphene, operating as a broadband image sensor has been realized, in which the graphene and the read-out circuit were connected with a vertical metal interconnect.^[307] The image sensor consists of a 388×288 array of graphene-quantum dot photodetectors and shows high sensitivity at visible and short-wave infrared band. Besides, in optoelectronic circuits, coupling 2D materials with in-plane evanescent field in an optical waveguide offers a new platform for exploring their potential use in optoelectronic integration. Photodetection in a 2D material/waveguide configuration has shown substantial advantages, especially in terms of low dark current and high responsivity.^[308–310] In these structures, the incident light is restricted and transmitted in the waveguide. The increase of the interaction length through light coupling between the 2D material and evanescent field in the optical waveguide, and a naturally formed 2D material/waveguide heterojunction affords a low dark current and significantly enhanced photoresponsivity. A graphene slot waveguide device features with compact footprint and enhanced light–matter interactions with the top graphene layer.^[311] A relatively high responsivity of 0.273 A W^{-1} was demonstrated at $1.55 \mu\text{m}$ wavelengths. A gated multilayer BP transistor integrated on a silicon waveguide was also demonstrated in the infrared telecommunication band.^[246] In a significant advantage over graphene/waveguide devices, this device can operate with lower dark current. And the device demonstrated responsivities of 657 mA W^{-1} using a 100 nm-thick BP, and a high bandwidth exceeding 3 GHz. A TMDCs based waveguide device was

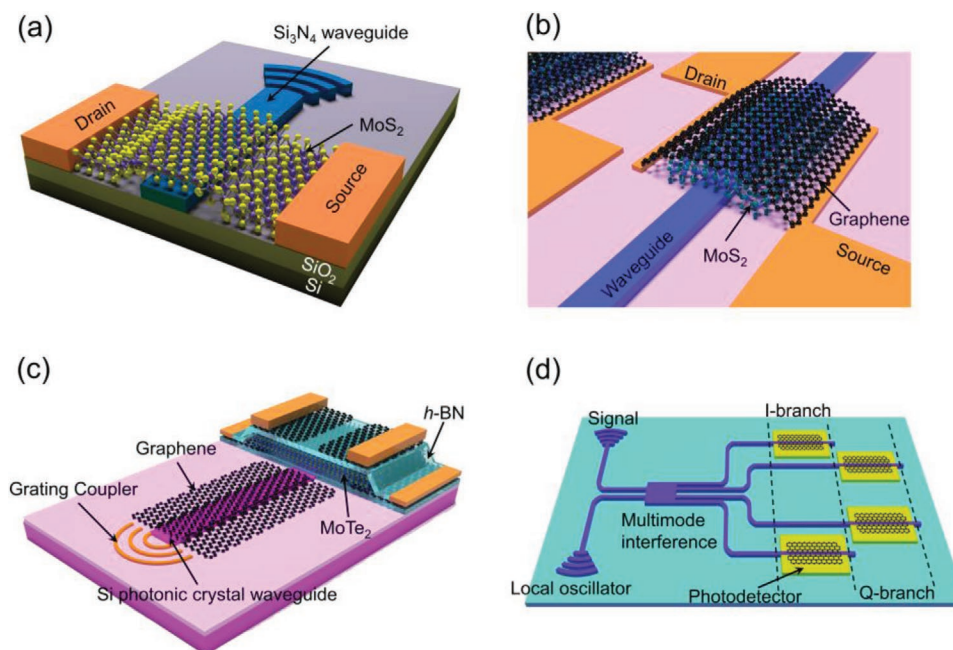


Figure 9. 2D materials integrated with silicon planar optoelectronics. a) schematics of the photodetector with monolayer MoS₂ directly integrated on top of the waveguide.^[312] b) Schematic diagram of integrating graphene/MoS₂ heterostructure with SiN₄ waveguide.^[313] c) Schematic of the waveguide-integrated MoTe₂ LED and photodetector.^[127] d) Schematic diagram of the proposed graphene-based optical coherent receiver.^[315]

also realized employing few-layer MoTe₂ as light absorption layer.^[309] Due to the strong light–matter interaction and sizable bandgap of MoTe₂, a very low dark current at nanoampere level and high-speed operation were achieved with no need of electrostatic gating, which simplifies the future integration of 2D materials with silicon photonics. The device demonstrated a photoresponse speed exceeding 500 MHz and optical data rates of 1 Gbits⁻¹, holding great potential for optical communication applications. The results provide a potential platform for integration of TMDCs with silicon photonic structures.

More recently, MoS₂ photodetector integrated with silicon photonic circuits was demonstrated, where MoS₂ can act as light absorption layer on silicon nitride waveguide, as demonstrated in **Figure 9a**.^[312] Efficient light absorption and photocurrent generation on integrated optical circuits was achieved in MoS₂. The light incident on the grating coupler can be directed to the waveguide and interact with the MoS₂ attached on top of the waveguide, leading to a large responsivity in MoS₂ for lateral illumination at wavelengths close to the optical bandgap. Besides, a TMDCs heterostructure integrated waveguide device was also realized by employing graphene and MoS₂ as light absorption layer (Figure 9b).^[313] The waveguide overlaps with the absorption layer and enhances the light–matter interactions with graphene/MoS₂ heterostructure. The photogenerated electron–hole pairs are produced at MoS₂ monolayer, and then rapidly separated at the heterostructure interface. The Fermi energy of graphene could be tuned by the back-gate voltage to get better performance at visible spectrum range. Furthermore, by realizing more complex structures, the use of TMDCs as a platform for integrated optoelectronic circuits, which combines light emission, optical interconnects and detection, was realized, as shown in Figure 9c.^[127] A p–n junction made of bilayer

MoTe₂ was integrated with silicon photonic-crystal waveguide and a grating coupler. The bilayer MoTe₂ on top of the waveguide works as both light emission source and photodetection layer. A layer of h-BN was used to protect the MoTe₂ from oxidation and separate it from the top gate electrodes. When the p–n junction works as light emitter, the light will propagate along the waveguide and emit at the grating coupler, while, when the device functions as a photodetector, the incident light couples into the waveguide and transforms into the electrical signal. This architecture shows that the active optical components for point-to-point interconnects are possible with 2D materials transferred onto otherwise passive photonic integrated circuits.

A chalcogenide glass (ChG), which has exceptional optical properties like broadband transparency, high and continuously tunable refractive indices and large Kerr nonlinearity, as the backbone optical material was present for photonic integration.^[314] The giant optical anisotropy of graphene and modal symmetry in graphene-sandwiched chalcogenide glass waveguides was exploited and demonstrated for integrated fabrication of ultra-broadband on-chip polarization isolation and thermo-optic switching. The devices show the record energy efficiency of a low switching energy of 0.11 mW, a 10–90% rise time of 14 μs, and a figure of merit of 0.65 mW⁻¹ μs⁻¹ which is among the highest values reported in an on-chip thermo-optic switch. Moreover, MIR graphene ChG waveguide-integrated broadband MIR detectors and modulators were realized by leveraging the zero-gap nature of graphene, where the multifunctional ChG material serves simultaneously as the waveguide and as a gate dielectric to electrostatically modulate the Fermi level in graphene. The devices exhibit a broadband photoresponse over the entire scanning range (2.0–2.55 μm) with a peak responsivity of 250 mA W⁻¹ at a wavelength of 2.03 μm

and a broadband optical modulation for the transverse electric (TE) mode across the 2.05–2.45 μm band with modulation depth up to 8 dB mm^{-1} . The versatile glass-on-2D-material platform will significantly expedite and expand integration of 2D materials to enable new photonic functionalities.

An integrated coherent light receiver chip composed of graphene photodetector and four channel-plasmonic slot waveguide was realized with ultrahigh-speed and high-quality reception for detecting advanced modulation formats that encode information on both the amplitude and phase of the light (Figure 9d).^[315] A 4×4 multimode interference coupler was used as a 90° optical hybrid, and it can realize the phase relationship of four channel output ports required by coherent optical receiver without the need of additional phase control unit. By using the graphene photodetector on the surface plasmon slot waveguide, the effective detection area of the graphene coherent light receiving chip is only $4 \mu\text{m} \times 15 \mu\text{m} \times 100 \text{ nm}$ with a responsivity of 0.1 A W^{-1} and a response bandwidth larger than 67 GHz. Combined with the balanced detection, 90 Gbits $^{-1}$ binary phase-shift keying signal is received with a promoted signal-to-noise ratio. Moreover, receptions of 200 Gbits $^{-1}$ quadrature phase-shift keying and 240 Gbits $^{-1}$ 16 quadrature amplitude modulation signals on a single-polarization carrier are realized with a low additional power consumption below 14 fJbit $^{-1}$. This graphene-based optical coherent receiver will promise potential applications in 400-Gigabit Ethernet and 800-Gigabit Ethernet technology, paving another route for future high-speed coherent optical communication networks.

9. Conclusion and Perspectives

In conclusion, tremendous efforts have been devoted on research of 2D materials, which has accelerated successful demonstrations of prototype optoelectronic devices based on them. The ultrathin body of 2D materials facilitates their integration

with silicon photonics which may revolutionize the future semiconductor technology. To date, the 2D material based optoelectronic devices including light sources, optical modulators, photodetectors, and transistors have been fabricated, and a few prototype structures of these devices with silicon photonics have been successfully demonstrated. Figure 10 depicts a potential scheme of 2D materials in the optoelectronic integration. Despite that they have shown many intriguing performance and advantages, the 2D materials based optoelectronic devices still have some challenges to resolve for the future use in optoelectronic integration.

For on-chip light emission, electrically pumped laser is preferred for on-chip integration. So far, most of the reported 2D materials based lasers are optically pumped despite that electrically pumped LEDs based on 2D materials have been realized. Lower threshold and higher output power may be achieved by optimizing the structure of the device, for instance, by integrated with photonic crystal cavity. The diversity of heterostructures which differs by stacking orientations, layer combinations, and tunable band alignment opens up more possibilities for constructing on-chip light sources in the future.

For optical modulation, despite of the successful demonstration of graphene-based electro-optic modulators, the modulation bandwidth was, however, generally limited by the response time of the bias circuit to ≈ 1 GHz. The main obstacle is arising from the resistance constant and limitation of the velocity speed of electrons. In comparison, thermo-optic modulator usually has narrower bandwidth and slower operation speed. Therefore, thermo-optic modulators are suitable for applications not requiring high speed, such as short-distance optical communication, optical routing, and switching. For future optical data processing, a modulation rate larger than 100 GHz is needed. Other high performance optical modulators based on 2D materials beyond graphene remain elusive so far and need further exploration.

For light detection, photodetectors based on 2D materials are extremely attractive in terms of their utility in photonic

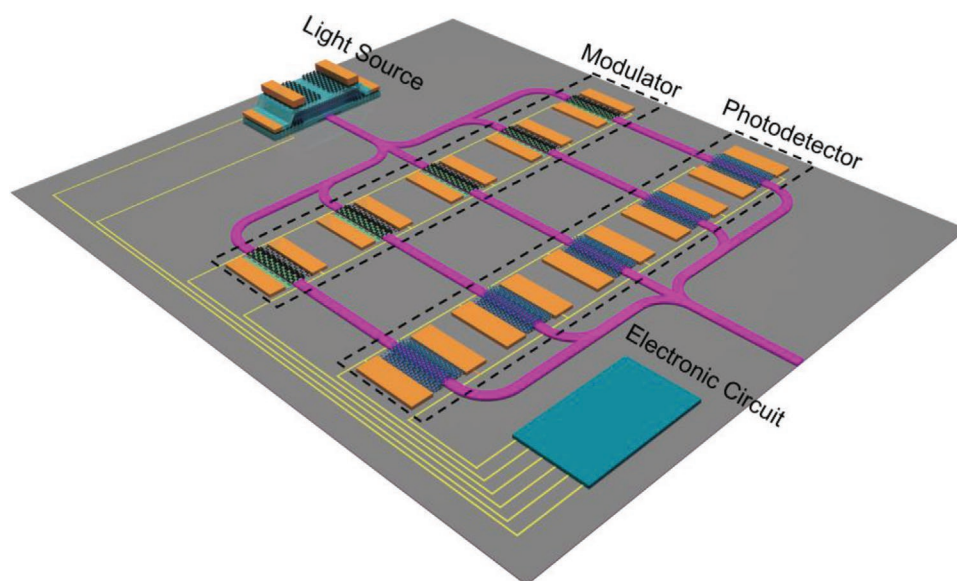


Figure 10. A representative diagram of 2D materials based optoelectronic integration.

technology, especially at infrared band, overcoming the difficulty of integrating silicon with traditional III–V semiconductor photodetectors. The use of graphene based photodetectors is strongly limited by the large dark currents when working in the photoconduction mode, or by the low responsivity when working in photovoltaic mode. Both of these situations mean the device could not respond at low levels of light intensity. The TMDCs based photodetectors suffer from narrow photoresponse range, and trap states that will greatly slow down its operation speed. In the future, the exploration of novel 2D materials and thus the creation of vdW heterostructures offers many possibilities to obtain unprecedented optoelectronic functionality and a novel platform for realizing high-performance photodetectors.

For energy-efficient integrated circuits application, in the future, exploration of high-quality dielectric layer is needed to achieve good interface features in 2D materials based electronic devices. Additionally, future work also involves thickness scaling of individual device down to a monolayer and the device channel length scaling down to the molecular-scale dimensions in order to obtain smaller device size and increase the integration of the devices. In silicon MOSFETs, compensating doping of a single active channel to form n-type and p-type regions is used to realize complementary logic circuits and reduce device power dissipation, but it is difficult to achieve in 2D materials, thereby vdW stacking could become a feasible solution to construct 2D complementary logic circuits.

Based on above discussions, 2D materials still face challenges in terms of practical application. These challenges may in turn present great opportunities in the research field. The large-scale production of high-quality 2D semiconducting materials is an important step toward its practical application. The development of wafer-scale fabrication technologies of vdW stacks of 2D materials is important in future. Although considerable progress has been made in the synthesis of ultrathin 2D materials and their related heterojunctions, a common problem for their synthesizing and processing technologies is the difficulty in fabricating continuous and homogeneous 2D crystals reproducibly at the wafer scale. The lateral dimensions of the products need to meet the current standards for mature semiconductor technologies, which are on a scale of centimeters. Even if large-area materials can be synthesized, the complete transfer to the substrate is still difficult, such as transferring wafer-scale h-BN on copper to silicon substrate. Besides, precise alignment between layers is also a great challenge especially when being moved from single device to on-chip integration. Modification is another important aspect of the development of 2D materials. Through doping, chemical modification, electrostatic control may resolve this problem. One more thing, the device stability must be addressed to achieve real applications. Due to their ultrathin characteristics, 2D materials are more susceptible to environmental circumstances. Thereby, how to protect 2D materials while reducing the influence on charge transport and optical properties is an important issue on the way toward real applications. For further optimization of device performances, the properties of existing 2D materials, especially heterojunctions, also can be further explored. With the continuous development of 2D materials and the improvement of experimental accuracy and controllability, researchers can explore and

develop new functionalities by regulating atomic composition and structure of 2D materials.

Acknowledgements

The authors acknowledge support from the National Natural Science Foundation of China (Grant Nos. 62022081 and 61974099) and the Science Fund for Creative Research Groups of the National Natural Science Foundation of China (62121005). Natural Science Foundation of Jilin Province (20210101173)C.

Conflict of Interest

The authors declare no conflict of interest.

Keywords

2D materials, electronic circuits, light sources, optical modulators, optoelectronic integration, photodetectors

Received: October 7, 2021

Revised: November 11, 2021

Published online: December 8, 2021

- [1] C. Sun, M. T. Wade, Y. Lee, J. S. Orcutt, L. Alloatti, M. S. Georgas, A. S. Waterman, J. M. Shainline, R. R. Avizienis, S. Lin, B. R. Moss, R. Kumar, F. Pavanello, A. H. Atabaki, H. M. Cook, A. J. Ou, J. C. Leu, Y.-H. Chen, K. Asanovic, R. J. Ram, M. A. Popovic, V. M. Stojanovic, *Nature* **2015**, 528, 534.
- [2] A. H. Atabaki, S. Moazeni, F. Pavanello, H. Gevorgyan, J. Notaros, L. Alloatti, M. T. Wade, C. Sun, S. A. Kruger, H. Y. Meng, K. Al Qubaisi, I. Wang, B. H. Zhang, A. Khilo, C. V. Baiocco, M. A. Popovic, V. M. Stojanovic, R. J. Ram, *Nature* **2018**, 556, 349.
- [3] C. Haffner, D. Chelladurai, Y. Fedoryshyn, A. Josten, B. Baeuerle, W. Heni, T. Watanabe, T. Cui, B. J. Cheng, S. Saha, D. L. Elder, L. R. Dalton, A. Boltasseva, V. M. Shalaev, N. Kinsey, J. Leuthold, *Nature* **2018**, 556, 483.
- [4] C. Wang, M. Zhang, X. Chen, M. Bertrand, A. Shams-Ansari, S. Chandrasekhar, P. Winzer, M. Loncar, *Nature* **2018**, 562, 101.
- [5] A. Mahmood, J. Y. Hu, B. Xiao, A. L. Tang, X. C. Wang, E. J. Zhou, *J. Mater. Chem. A* **2018**, 6, 16769.
- [6] A. Takshi, H. Yaghoubi, D. I. Jun, J. T. Beatty, *Electronics* **2020**, 9, 1709.
- [7] L. Suresh, J. V. Vaghiasya, D. K. Nandakumar, T. F. Wu, M. R. Jones, S. C. Tan, *Chem* **2019**, 5, 1847.
- [8] S. K. Ravi, Z. M. Yu, D. J. K. Swainsbury, J. Y. Ouyang, M. R. Jones, S. C. Tan, *Adv. Energy Mater.* **2017**, 7, 1601821.
- [9] K. Hajdu, R. F. Balderas-Valadez, A. Carlino, V. Agarwal, L. Nagy, *Photochem. Photobiol. Sci.* <https://doi.org/10.1007/s43630-021-00121-y>.
- [10] S. K. Ravi, Y. X. Zhang, Y. N. Wang, D. K. Nandakumar, W. X. Sun, M. R. Jones, S. C. Tan, *Adv. Energy Mater.* **2019**, 9, 1901449.
- [11] D. S. Liu, J. Wu, H. X. Xu, Z. M. Wang, *Adv. Mater.* **33**, 2003733.
- [12] Y. Liu, X. D. Duan, H. J. Shin, S. Park, Y. Huang, X. F. Duan, *Nature* **2021**, 591, 43.
- [13] Q. X. Qiu, Z. M. Huang, *Adv. Mater.* **2021**, 33, 2008126.
- [14] Z. P. Sun, A. Martinez, F. Wang, *Nat. Photonics* **2016**, 10, 227.
- [15] K. S. Novoselov, A. K. Geim, S. Morozov, D. Jiang, Y. Zhang, S. Dubonos, I. Grigorieva, A. Firsov, *Science* **2004**, 306, 666.

- [16] K. S. Novoselov, D. Jiang, F. Schedin, T. J. Booth, V. V. Khotkevich, S. V. Morozov, A. K. Geim, *Proc. Natl. Acad. Sci. USA* **2005**, *102*, 10451.
- [17] A. C. Neto, F. Guinea, N. Peres, K. S. Novoselov, A. K. Geim, *Rev. Mod. Phys.* **2009**, *81*, 109.
- [18] Q. Bao, K. P. Loh, *ACS Nano* **2012**, *6*, 3677.
- [19] M. Buscema, D. J. Groenendijk, S. I. Blanter, G. A. Steele, H. S. van der Zant, A. Castellanos-Gomez, *Nano Lett.* **2014**, *14*, 3347.
- [20] P. Hu, Z. Wen, L. Wang, P. Tan, K. Xiao, *ACS Nano* **2012**, *6*, 5988.
- [21] L. Huang, B. W. Dong, X. Guo, Y. H. Chang, N. Chen, X. Huang, W. G. Liao, C. X. Zhu, H. Wang, C. Lee, K. W. Ang, *ACS Nano* **2019**, *13*, 913.
- [22] Q. J. Liang, Q. X. Wang, Q. Zhang, J. X. Wei, S. X. D. Lim, R. Zhu, J. X. Hu, W. Wei, C. Lee, C. Sow, W. J. Zhang, A. T. S. Wee, *Adv. Mater.* **2019**, *31*, 1807609.
- [23] X. C. Yu, P. Yu, D. Wu, B. Singh, Q. S. Zeng, H. Lin, W. Zhou, J. H. Lin, K. Suenaga, Z. Liu, Q. J. Wang, *Nat. Commun.* **2018**, *9*, 1545.
- [24] M. Liu, X. Yin, E. Ulin-Avila, B. Geng, T. Zentgraf, L. Ju, F. Wang, X. Zhang, *Nature* **2011**, *474*, 64.
- [25] Y. Yamaguchi, S. Takagi, M. Takenaka, *Jpn. J. Appl. Phys.* **2018**, *57*, 04FH06.
- [26] H. Tian, M. L. Chin, S. Najmaei, Q. S. Guo, F. N. Xia, H. Wang, M. Dubey, *Nano Res.* **2016**, *9*, 1543.
- [27] R. Frisenda, A. J. Molina-Mendoza, T. Mueller, A. Castellanos-Gomez, H. S. J. van der Zant, *Chem. Soc. Rev.* **2018**, *47*, 3339.
- [28] X. T. Yu, X. Wang, F. F. Zhou, J. L. Qu, J. Song, *Adv. Funct. Mater.* **2021**, *31*, 2104260.
- [29] S. J. Liang, B. Cheng, X. Y. Cui, F. Miao, *Adv. Mater.* **2020**, *32*, 1903800.
- [30] P. Wang, H. Xia, Q. Li, F. Wang, L. L. Zhang, T. X. Li, P. Martyniuk, A. Rogaiski, W. D. Hu, *Small* **2019**, *15*, 1904396.
- [31] J. Z. Fang, Z. Q. Zhou, M. Q. Xiao, Z. Lou, Z. M. Wei, G. Z. Shen, *InfoMat* **2020**, *2*, 291.
- [32] X. T. Wang, Y. Cui, T. Li, M. Lei, J. B. Li, Z. M. Wei, *Adv. Opt. Mater.* **2019**, *7*, 1801274.
- [33] F. Liu, *Prog. Surf. Sci.* **2021**, *96*, 100626.
- [34] Y. Huang, Y. H. Pan, R. Yang, L. H. Bao, L. Meng, H. L. Luo, Y. Q. Cai, G. D. Liu, W. J. Zhao, Z. Zhou, L. M. Wu, Z. L. Zhu, M. Huang, L. W. Liu, L. Liu, P. Cheng, K. H. Wu, S. B. Tian, C. Z. Gu, Y. G. Shi, Y. F. Guo, Z. G. Cheng, J. P. Hu, L. Zhao, G. H. Yang, E. Sutter, P. Sutter, Y. L. Wang, W. Ji, X. J. Zhou, H. J. Gao, *Nat. Commun.* **2020**, *11*, 2453.
- [35] F. I. Alzackia, S. C. Tan, *Adv. Sci.* **2021**, *8*, 2003864.
- [36] F. I. Alzackia, W. Jonhson, J. Ding, S. C. Tan, *ACS Appl. Mater. Interfaces* **2020**, *12*, 28840.
- [37] H. C. Tao, Y. Q. Zhang, Y. N. Gao, Z. Y. Sun, C. Yan, J. Texter, *Phys. Chem. Chem. Phys.* **2017**, *19*, 921.
- [38] Z. H. Wang, F. Li, J. Guo, C. Y. Ma, Y. F. Song, Z. W. He, J. Liu, Y. P. Zhang, D. L. Li, H. Zhang, *Adv. Opt. Mater.* **2020**, *8*, 1902183.
- [39] M. El Garah, S. Bertolazzi, S. Ippolito, M. Eredia, I. Janica, G. Melinte, O. Ersen, G. Marletta, A. Ciesielski, P. Samori, *FlatChem* **2018**, *9*, 33.
- [40] X. Fan, P. Xu, D. Zhou, Y. Sun, Y. C. Li, M. A. T. Nguyen, M. Terrones, T. E. Mallouk, *Nano Lett.* **2015**, *15*, 5956.
- [41] R. Ikram, B. M. Jan, W. Ahmad, *J. Mater. Res. Technol.* **2020**, *9*, 11587.
- [42] L. Li, D. Zhang, J. P. Deng, Q. Kang, Z. F. Liu, J. F. Fang, Y. C. Gou, *J. Electrochem. Soc.* **2020**, *167*, 155519.
- [43] B. Deng, Z. F. Liu, H. L. Peng, *Adv. Mater.* **2019**, *31*, 1800996.
- [44] Z. Y. Cai, B. L. Liu, X. L. Zou, H. M. Cheng, *Chem. Rev.* **2018**, *118*, 6091.
- [45] M. Jana, R. N. Singh, *Int. Mater. Rev.* **2018**, *63*, 162.
- [46] M. Huang, B. W. Deng, F. Dong, L. L. Zhang, Z. Y. Zhang, P. Chen, *Small Methods* **2021**, *5*, 2001213.
- [47] Y. X. Fan, L. Li, G. Yu, D. C. Geng, X. T. Zhang, W. P. Hu, *Adv. Mater.* **2021**, *33*, 2003956.
- [48] J. Wang, T. Li, Q. Wang, W. Wang, R. Shi, N. Wang, A. Amini, C. Cheng, *Mater. Today Adv.* **2020**, *8*, 100098.
- [49] H. Li, Y. Li, A. Aljarb, Y. Shi, L.-J. Li, *Chem. Rev.* **2018**, *118*, 6134.
- [50] B. Qin, H. F. Ma, M. Hossain, M. Z. Zhong, Q. L. Xia, B. Li, X. D. Duan, *Chem. Mater.* **2020**, *32*, 10321.
- [51] T. F. Schranghamer, M. Sharma, R. Singh, S. Das, *Chem. Soc. Rev.* **2021**, *50*, 11032.
- [52] Y. Q. Song, W. T. Zou, Q. Lu, L. Lin, Z. F. Liu, *Small* **2021**, <https://doi.org/10.1002/sml.202007600>.
- [53] Q. Liu, X. S. Wang, J. L. Wang, X. Huang, *Acta Phys.-Chim. Sin.* **2019**, *35*, 1099.
- [54] X. L. Xu, Y. Pan, S. Liu, B. Han, P. F. Gu, S. H. Li, W. J. Xu, Y. X. Peng, Z. Han, J. Chen, P. Gao, Y. Ye, *Science* **2021**, *372*, 195.
- [55] C. Liu, X. Z. Xu, L. Qiu, M. H. Wu, R. X. Qiao, L. Wang, J. H. Wang, J. J. Niu, J. Liang, X. Zhou, Z. H. Zhang, M. Peng, P. Gao, W. L. Wang, X. D. Bai, D. Ma, Y. Jiang, X. S. Wu, D. P. Yu, E. G. Wang, J. Xiong, F. Ding, K. H. Liu, *Nat. Chem.* **2019**, *11*, 730.
- [56] L. Wang, X. Z. Xu, L. N. Zhang, R. X. Qiao, M. H. Wu, Z. C. Wang, S. Zhang, J. Liang, Z. H. Zhang, Z. B. Zhang, W. Chen, X. D. Xie, J. Y. Zong, Y. W. Shan, Y. Guo, M. Willinger, H. Wu, Q. Y. Li, W. L. Wang, P. Gao, S. W. Wu, Y. Zhang, Y. Jiang, D. P. Yu, E. G. Wang, X. D. Bai, Z. J. Wang, F. Ding, K. H. Liu, *Nature* **2019**, *570*, 91.
- [57] J. D. Zhou, J. H. Lin, X. W. Huang, Y. Zhou, Y. Chen, J. Xia, H. Wang, Y. Xie, H. M. Yu, J. C. Lei, D. Wu, F. C. Liu, Q. D. Fu, Q. S. Zeng, C. H. Hsu, C. L. Yang, L. Lu, T. Yu, Z. X. Shen, H. Lin, B. I. Yakobson, Q. Liu, K. Suenaga, G. T. Liu, Z. Liu, *Nature* **2018**, *556*, 355.
- [58] L. N. Liu, J. X. Wu, L. Y. Wu, M. Ye, X. Z. Liu, Q. Wang, S. Y. Hou, P. F. Lu, L. F. Sun, J. Y. Zheng, L. Xing, L. Gu, X. W. Jiang, L. M. Xie, L. Y. Jiao, *Nat. Mater.* **2018**, *17*, 1108.
- [59] M. Sang, J. Shin, K. Kim, K. J. Yu, *Nanomaterials* **2019**, *9*, 374.
- [60] J. G. Wang, X. J. Mu, M. T. Sun, *Nanomaterials* **2019**, *9*, 218.
- [61] R. G. Ma, Y. Zhou, H. Bi, M. H. Yang, J. C. Wang, Q. Liu, F. Q. Huang, *Prog. Mater. Sci.* **2020**, *113*, 100665.
- [62] F. Wang, Y. B. Zhang, C. S. Tian, C. Girit, A. Zettl, M. Crommie, Y. R. Shen, *Science* **2008**, *320*, 206.
- [63] M. Yu, C. Chen, Q. Liu, C. Mattioli, H. Sang, G. Shi, W. Huang, K. Shen, Z. Li, P. Ding, P. Guan, S. Wang, Y. Sun, J. Hu, A. Gourdon, L. Kantorovich, F. Besenbacher, M. Chen, F. Song, F. Rosei, *Nat. Chem.* **2020**, *12*, 1035.
- [64] S. Y. Lee, D. D. Loc, V. Q. An, Y. Jin, P. Kim, Y. H. Lee, *ACS Nano* **2015**, *9*, 9034.
- [65] Y. Qu, J. Ding, H. Fu, H. Chen, J. Peng, *Appl. Surf. Sci.* **2021**, *542*, 148763.
- [66] F. Guinea, M. I. Katsnelson, A. K. Geim, *Nat. Phys.* **2010**, *6*, 30.
- [67] V. M. Pereira, A. H. Castro Neto, N. M. R. Peres, *Phys. Rev. B* **2009**, *80*, 045401.
- [68] Y. Zhang, T.-T. Tang, C. Girit, Z. Hao, M. C. Martin, A. Zettl, M. F. Crommie, Y. R. Shen, F. Wang, *Nature* **2009**, *459*, 820.
- [69] F. Xia, D. B. Farmer, Y.-m. Lin, P. Avouris, *Nano Lett.* **2010**, *10*, 715.
- [70] T. Ohta, A. Bostwick, T. Seyller, K. Horn, E. Rotenberg, *Science* **2006**, *313*, 951.
- [71] S. H. Kang, W. S. Hwang, Z. Lin, S. H. Kwon, S. W. Hong, *Nano Lett.* **2015**, *15*, 7913.
- [72] M. Y. Han, B. Oezylmaz, Y. Zhang, P. Kim, *Phys. Rev. Lett.* **2007**, *98*, 206805.
- [73] X. Wang, Y. Ouyang, X. Li, H. Wang, J. Guo, H. Dai, *Phys. Rev. Lett.* **2008**, *100*, 206803.
- [74] F. Ke, Y. B. Chen, K. T. Yin, J. J. Yan, H. Z. Zhang, Z. X. Liu, J. S. Tse, J. Q. Wu, H. K. Mao, B. Chen, *Proc. Natl. Acad. Sci. USA* **2019**, *116*, 9186.

- [75] H. Sakaguchi, Y. Kawagoe, Y. Hirano, T. Iruka, M. Yano, T. Nakae, *Adv. Mater.* **2014**, *26*, 4134.
- [76] J. M. Cai, P. Ruffieux, R. Jaafar, M. Bieri, T. Braun, S. Blankenburg, M. Muoth, A. P. Seitsonen, M. Saleh, X. L. Feng, K. Mullen, R. Fasel, *Nature* **2010**, *466*, 470.
- [77] J. M. Cai, C. A. Pignedoli, L. Talirz, P. Ruffieux, H. Sode, L. B. Liang, V. Meunier, R. Berger, R. J. Li, X. L. Feng, K. Mullen, R. Fasel, *Nat. Nanotechnol.* **2014**, *9*, 896.
- [78] P. Ruffieux, J. M. Cai, N. C. Plumb, L. Patthey, D. Prezzi, A. Ferretti, E. Molinari, X. L. Feng, K. Mullen, C. A. Pignedoli, R. Fasel, *ACS Nano* **2012**, *6*, 6930.
- [79] Y. C. Chen, D. G. de Oteyza, Z. Pedramrazi, C. Chen, F. R. Fischer, M. F. Crommie, *ACS Nano* **2013**, *7*, 6123.
- [80] H. M. Zhang, H. P. Lin, K. W. Sun, L. Chen, Y. Zagranyarski, N. Aghdassi, S. Duhm, Q. Li, D. Y. Zhong, Y. Y. Li, K. Mullen, H. Fuchs, L. F. Chi, *J. Am. Chem. Soc.* **2015**, *137*, 4022.
- [81] A. F. Rigosi, A. L. Levy, M. R. Snure, N. R. Glavin, *J. Phys. Mater.* **2021**, *4*, 032003.
- [82] Y. N. Gong, Z. Q. Xu, D. L. Li, J. Zhang, I. Aharonovich, Y. P. Zhang, *ACS Energy Lett.* **2021**, *6*, 985.
- [83] H. L. Lu, Y. Y. Zhang, X. Lin, H. J. Gao, *Sci. China: Phys., Mech. Astron.* **2021**, *64*, 106801.
- [84] B. Zhao, D. Y. Shen, Z. C. Zhang, P. Lu, M. Hossain, J. Li, B. Li, X. D. Duan, *Adv. Funct. Mater.* **2021**, *31*, 2105132.
- [85] W. J. Zhu, T. Low, H. Wang, P. D. Ye, X. F. Duan, *2D Mater.* **2019**, *6*, 032004.
- [86] M. K. Wang, J. Zhu, Y. Zi, Z. G. Wu, H. G. Hu, Z. J. Xie, Y. Zhang, L. P. Hu, W. C. Huang, *J. Mater. Chem. A* **2021**, *9*, 12433.
- [87] Y. Yi, Z. B. Sun, J. Li, P. K. Chu, X. F. Yu, *Small Methods* **2019**, *3*, 1900165.
- [88] J. S. Miao, L. Zhang, C. Wang, *2D Mater.* **2019**, *6*, 032003.
- [89] M. Galbiati, N. Motta, M. De Crescenzi, L. Camilli, *Appl. Phys. Rev.* **2019**, *6*, 041310.
- [90] N. N. Liu, G. Y. Bo, Y. N. Liu, X. Xu, Y. Du, S. X. Dou, *Small* **2019**, *15*, 1805147.
- [91] S. Y. Guo, Y. P. Zhang, Y. Q. Ge, S. L. Zhang, H. B. Zeng, H. Zhang, *Adv. Mater.* **2019**, *31*, 1902352.
- [92] X. Wang, X. T. Yu, J. Song, W. C. Huang, Y. J. Xiang, X. Y. Dai, H. Zhang, *Chem. Eng. J.* **2021**, *406*, 126876.
- [93] M. F. Tuo, C. Xu, H. R. Mu, X. Z. Bao, Y. W. Wang, S. Xiao, W. L. Ma, L. Li, D. Y. Tang, H. Zhang, M. Premaratne, B. Q. Sun, H. M. Cheng, S. J. Li, W. C. Ren, Q. L. Bao, *ACS Photonics* **2018**, *5*, 1808.
- [94] Y. Gutierrez, P. Garcia-Fernandez, J. Junquera, A. S. Brown, F. Moreno, M. Losurdo, *Nanophotonics* **2020**, *9*, 4233.
- [95] D. Golberg, Y. Bando, Y. Huang, T. Terao, M. Mitome, C. C. Tang, C. Y. Zhi, *ACS Nano* **2010**, *4*, 2979.
- [96] L. Song, L. J. Ci, H. Lu, P. B. Sorokin, C. H. Jin, J. Ni, A. G. Kvashnin, D. G. Kvashnin, J. Lou, B. I. Yakobson, P. M. Ajayan, *Nano Lett.* **2010**, *10*, 3209.
- [97] C. R. Dean, A. F. Young, I. Meric, C. Lee, L. Wang, S. Sorgenfrei, K. Watanabe, T. Taniguchi, P. Kim, K. L. Shepard, J. Hone, *Nat. Nanotechnol.* **2010**, *5*, 722.
- [98] M. Q. Zeng, J. X. Liu, L. Zhou, R. G. Mendes, Y. Q. Dong, M. Y. Zhang, Z. H. Cui, Z. H. Cai, Z. Zhang, D. M. Zhu, T. Y. Yang, X. L. Li, J. Q. Wang, L. Zhao, G. X. Chen, H. Jiang, M. H. Rummeli, H. Zhou, L. Fu, *Nat. Mater.* **2020**, *19*, 528.
- [99] K. F. Mak, J. Shan, *Nat. Photonics* **2016**, *10*, 216.
- [100] D. Jariwala, V. K. Sangwan, L. J. Lauhon, T. J. Marks, M. C. Hersam, *ACS Nano* **2014**, *8*, 1102.
- [101] S. Das, W. Zhang, M. Demarteau, A. Hoffmann, M. Dubey, A. Roelofs, *Nano Lett.* **2014**, *14*, 5733.
- [102] L. Li, Y. Yu, G. J. Ye, Q. Ge, X. Ou, H. Wu, D. Feng, X. H. Chen, Y. Zhang, *Nat. Nanotechnol.* **2014**, *9*, 372.
- [103] S. Zhang, Z. Yan, Y. Li, Z. Chen, H. Zeng, *Angew. Chem., Int. Ed.* **2015**, *54*, 3112.
- [104] L. T. Dou, A. B. Wong, Y. Yu, M. L. Lai, N. Kornienko, S. W. Eaton, A. Fu, C. G. Bischak, J. Ma, T. N. Ding, N. S. Ginsberg, L. W. Wang, A. P. Alivisatos, P. D. Yang, *Science* **2015**, *349*, 1518.
- [105] J. Y. Liu, Y. Z. Xue, Z. Y. Wang, Z. Q. Xu, C. X. Zheng, B. Weber, J. C. Song, Y. S. Wang, Y. R. Lu, Y. P. Zhang, Q. L. Bao, *ACS Nano* **2016**, *10*, 3536.
- [106] A. K. Geim, I. V. Grigorieva, *Nature* **2013**, *499*, 419.
- [107] G. F. Rao, X. P. Wang, Y. Wang, P. H. Wangyang, C. Y. Yan, J. W. Chu, L. X. Xue, C. H. Gong, J. W. Huang, J. Xiong, Y. R. Li, *InfoMat* **2019**, *1*, 272.
- [108] Z. Wu, W. Jie, Z. Yang, J. Hao, *Mater. Today Nano* **2020**, *12*, 100092.
- [109] F. Withers, O. Del Pozo-Zamudio, A. Mishchenko, A. P. Rooney, A. Gholinia, K. Watanabe, T. Taniguchi, S. J. Haigh, A. K. Geim, A. I. Tartakovskii, K. S. Novoselov, *Nat. Mater.* **2015**, *14*, 301.
- [110] C. Gong, H. J. Zhang, W. H. Wang, L. Colombo, R. M. Wallace, K. J. Cho, *Appl. Phys. Lett.* **2013**, *103*, 053513.
- [111] M. Z. Bellus, F. Ceballos, H. Y. Chiu, H. Zhao, *ACS Nano* **2015**, *9*, 6459.
- [112] Y. P. An, Y. S. Hou, K. Wang, S. J. Gong, C. L. Ma, C. X. Zhao, T. X. Wang, Z. Y. Jiao, H. Y. Wang, R. Q. Wu, *Adv. Funct. Mater.* **2020**, *30*, 2002939.
- [113] W. Xin, X.-K. Li, X.-L. He, B.-W. Su, X.-Q. Jiang, K.-X. Huang, X.-F. Zhou, Z.-B. Liu, J.-G. Tian, *Adv. Mater.* **2018**, *30*, 1704653.
- [114] K. S. Novoselov, A. Mishchenko, A. Carvalho, A. H. C. Neto, *Science* **2016**, *353*, aac9439.
- [115] B. Fallahzad, K. Lee, S. Kang, J. M. Xue, S. Larentis, C. Corbet, K. Kim, H. C. P. Movva, T. Taniguchi, K. Watanabe, L. F. Register, S. K. Banerjee, E. Tutuc, *Nano Lett.* **2015**, *15*, 428.
- [116] J. Gaskell, L. Eaves, K. S. Novoselov, A. Mishchenko, A. K. Geim, T. M. Fromhold, M. T. Greenaway, *Appl. Phys. Lett.* **2015**, *107*, 103105.
- [117] F. He, Y. J. Zhou, Z. F. Ye, S. H. Cho, J. Jeong, X. H. Meng, Y. G. Wang, *ACS Nano* **2021**, *15*, 5944.
- [118] K. W. Tang, W. H. Qi, *Adv. Funct. Mater.* **2020**, *30*, 2002672.
- [119] Y. P. Liu, S. Y. Zhang, J. He, Z. M. M. Wang, Z. W. Liu, *Nano-Micro Lett.* **2019**, *11*, 13.
- [120] J. B. Cheng, C. L. Wang, X. M. Zou, L. Liao, *Adv. Opt. Mater.* **2019**, *7*, 1800441.
- [121] C. Hu, X. J. Wang, B. Song, *Light: Sci. Appl.* **2020**, *9*, 88.
- [122] M. Freitag, H.-Y. Chiu, M. Steiner, V. Perebeinos, P. Avouris, *Nat. Nanotechnol.* **2010**, *5*, 497.
- [123] Y. D. Kim, H. Kim, Y. Cho, J. H. Ryoo, C.-H. Park, P. Kim, Y. S. Kim, S. Lee, Y. Li, S.-N. Park, Y. S. Yoo, D. Yoon, V. E. Dorgan, E. Pop, T. F. Heinz, J. Hone, S.-H. Chun, H. Cheong, S. W. Lee, M.-H. Bae, Y. D. Park, *Nat. Nanotechnol.* **2015**, *10*, 676.
- [124] Y. D. Kim, Y. Gao, R.-J. Shiue, L. Wang, O. B. Aslan, M.-H. Bae, H. Kim, D. Seo, H.-J. Choi, S. H. Kim, A. Nemilentsau, T. Low, C. Tan, D. K. Efetov, T. Taniguchi, K. Watanabe, K. L. Shepard, T. F. Heinz, D. Englund, J. Hone, *Nano Lett.* **2018**, *18*, 934.
- [125] L. Dobusch, S. Schuler, V. Perebeinos, T. Mueller, *Adv. Mater.* **2017**, *29*, 1701304.
- [126] R. S. Sundaram, M. Engel, A. Lombardo, R. Krupke, A. C. Ferrari, P. Avouris, M. Steiner, *Nano Lett.* **2013**, *13*, 1416.
- [127] Y.-Q. Bie, G. Grosso, M. Heuck, M. M. Furchi, Y. Cao, J. Zheng, D. Bunandar, E. Navarro-Moratalla, L. Zhou, D. K. Efetov, T. Taniguchi, K. Watanabe, J. Kong, D. Englund, P. Jarillo-Herrero, *Nat. Nanotechnol.* **2017**, *12*, 1124.
- [128] R. Cheng, D. Li, H. Zhou, C. Wang, A. Yin, S. Jiang, Y. Liu, Y. Chen, Y. Huang, X. Duan, *Nano Lett.* **2014**, *14*, 5590.
- [129] G. Clark, J. R. Schaibley, J. Ross, T. Taniguchi, K. Watanabe, J. R. Hendrickson, S. Mou, W. Yao, X. Xu, *Nano Lett.* **2016**, *16*, 3944.
- [130] C. P. Berraquero, M. Barbone, D. M. Kara, X. Chen, I. Goykhman, D. Yoon, A. K. Ott, J. Beitner, K. Watanabe, T. Taniguchi, A. C. Ferrari, M. Atatüre, *Nat. Commun.* **2016**, *7*, 12978.

- [131] F. Xia, H. Wang, D. Xiao, M. Dubey, A. Ramasubramaniam, *Nat. Photonics* **2014**, *8*, 899.
- [132] C.-H. Liu, G. Clark, T. Fryett, S. Wu, J. Zheng, F. Hatami, X. Xu, A. Majumdar, *Nano Lett.* **2017**, *17*, 200.
- [133] D. N. M. Hanh, Z.-Q. Xu, M. Kianinia, R. Su, Z. Liu, S. Kim, C. Bradac, T. T. Trong, Y. Wan, L.-J. Li, A. Solntsev, J. Liu, I. Aharonovich, *ACS Photonics* **2018**, *5*, 3950.
- [134] Y. Ye, Z. J. Wong, X. Lu, X. Ni, H. Zhu, X. Chen, Y. Wang, X. Zhang, *Nat. Photonics* **2015**, *9*, 733.
- [135] O. Salehzadeh, M. Djavid, N. H. Tran, I. Shih, Z. Mi, *Nano Lett.* **2015**, *15*, 5302.
- [136] J. Shang, C. Cong, Z. Wang, N. Peimyoo, L. Wu, C. Zou, Y. Chen, X. Y. Chin, J. Wang, C. Soci, W. Huang, T. Yu, *Nat. Commun.* **2017**, *8*, 543.
- [137] Y. Li, J. Zhang, D. Huang, H. Sun, F. Fan, J. Feng, Z. Wang, C. Z. Ning, *Nat. Nanotechnol.* **2017**, *12*, 987.
- [138] H. Fang, J. Liu, H. Li, L. Zhou, L. Liu, J. Li, X. Wang, T. F. Krauss, Y. Wang, *Laser Photonics Rev.* **2018**, *12*, 1800015.
- [139] Y. Liu, H. Fang, A. Rasmita, Y. Zhou, J. Li, T. Yu, Q. Xiong, N. Zheludev, J. Liu, W. Gao, *Sci. Adv.* **2019**, *5*, eaav4506.
- [140] Z.-K. Tan, R. S. Moghaddam, M. L. Lai, P. Docampo, R. Higgler, F. Deschler, M. Price, A. Sadhanala, L. M. Pazos, D. Credgington, F. Hanusch, T. Bein, H. J. Snaith, R. H. Friend, *Nat. Nanotechnol.* **2014**, *9*, 687.
- [141] M. Ban, Y. Zou, J. P. H. Rivett, Y. Yang, T. H. Thomas, Y. Tan, T. Song, X. Gao, D. Credgington, F. Deschler, H. Sirringhaus, B. Sun, *Nat. Commun.* **2018**, *9*, 3892.
- [142] Z. Li, Z. Chen, Y. Yang, Q. Xue, H.-L. Yip, Y. Cao, *Nat. Commun.* **2019**, *10*, 1027.
- [143] M. J. Yuan, L. N. Quan, R. Comin, G. Walters, R. Sabatini, O. Voznyy, S. Hoogland, Y. B. Zhao, E. M. Beaugard, P. Kanjanaboos, Z. H. Lu, D. H. Kim, E. H. Sargent, *Nat. Nanotechnol.* **2016**, *11*, 872.
- [144] Y. Cao, N. N. Wang, H. Tian, J. S. Guo, Y. Q. Wei, H. Chen, Y. F. Miao, W. Zou, K. Pan, Y. R. He, H. Cao, Y. Ke, M. M. Xu, Y. Wang, M. Yang, K. Du, Z. W. Fu, D. C. Kong, D. X. Dai, Y. Z. Jin, G. Q. Li, H. Li, Q. M. Peng, J. P. Wang, W. Huang, *Nature* **2018**, *562*, 249.
- [145] K. B. Lin, J. Xing, L. N. Quan, F. P. G. de Arquer, X. W. Gong, J. X. Lu, L. Q. Xie, W. J. Zhao, D. Zhang, C. Z. Yan, W. Q. Li, X. Y. Liu, Y. Lu, J. Kirman, E. H. Sargent, Q. H. Xiong, Z. H. Wei, *Nature* **2018**, *562*, 245.
- [146] E. O. Polat, C. Kocabas, *Nano Lett.* **2013**, *13*, 5851.
- [147] A. Mahigir, G. Veronis, *J. Opt. Soc. Am. B* **2018**, *35*, 3153.
- [148] B. B. Zeng, Z. Q. Huang, A. Singh, Y. Yao, A. K. Azad, A. D. Mohite, A. J. Taylor, D. R. Smith, H. T. Chen, *Light: Sci. Appl.* **2018**, *7*, 51.
- [149] Y. Wu, C. La-o-Vorakiat, X. Qiu, J. Liu, P. Deorani, K. Banerjee, J. Son, Y. Chen, E. E. M. Chia, H. Yang, *Adv. Mater.* **2015**, *27*, 1874.
- [150] D. S. Jessop, S. J. Kindness, L. Xiao, P. Braeuninger-Weimer, H. Lin, Y. Ren, C. X. Ren, S. Hofmann, J. A. Zeitler, H. E. Beere, D. A. Ritchie, R. Degl'Innocenti, *Appl. Phys. Lett.* **2016**, *108*, 171101.
- [151] C. T. Phare, Y. H. D. Lee, J. Cardenas, M. Lipson, *Nat. Photonics* **2015**, *9*, 511.
- [152] K. Kim, J.-Y. Choi, T. Kim, S.-H. Cho, H.-J. Chung, *Nature* **2011**, *479*, 338.
- [153] C. Y. Qiu, W. L. Gao, R. Vajtai, P. M. Ajayan, J. Kono, Q. F. Xu, *Nano Lett.* **2014**, *14*, 6811.
- [154] B. C. Yao, S. W. Huang, Y. Liu, A. K. Vinod, C. Choi, M. Hoff, Y. N. Li, M. B. Yu, Z. Y. Feng, D. L. Kwong, Y. Huang, Y. J. Rao, X. F. Duan, C. W. Wong, *Nature* **2018**, *558*, 410.
- [155] S. Gan, C. T. Cheng, Y. H. Zhan, B. J. Huang, X. T. Gan, S. J. Li, S. H. Lin, X. F. Li, J. L. Zhao, H. D. Chen, Q. L. Bao, *Nanoscale* **2015**, *7*, 20249.
- [156] A. Alduino, M. Paniccia, *Nat. Photonics* **2007**, *1*, 153.
- [157] W. Li, B. G. Chen, C. Meng, W. Fang, Y. Xiao, X. Y. Li, Z. F. Hu, Y. X. Xu, L. M. Tong, H. Q. Wang, W. T. Liu, J. M. Bao, Y. R. Shen, *Nano Lett.* **2014**, *14*, 955.
- [158] J. A. Dionne, K. Diest, L. A. Sweatlock, H. A. Atwater, *Nano Lett.* **2009**, *9*, 897.
- [159] A. Emboras, J. Niegemann, P. Ma, C. Haffner, A. Pedersen, M. Luisier, C. Hafner, T. Schimmel, J. Leuthold, *Nano Lett.* **2016**, *16*, 709.
- [160] B. Huang, W. Lu, Z. Liu, S. Gao, *Opt. Express* **2018**, *26*, 7358.
- [161] Z. Fei, A. Rodin, G. Andreev, W. Bao, A. McLeod, M. Wagner, L. Zhang, Z. Zhao, M. Thiemens, G. Dominguez, *Nature* **2012**, *487*, 82.
- [162] J. Chen, M. Badioli, P. Alonso-Gonzalez, S. Thongrattanasiri, F. Huth, J. Osmond, M. Spasenovic, A. Centeno, A. Pesquera, P. Godignon, A. Z. Elorza, N. Camara, F. J. Garcia de Abajo, R. Hillenbrand, F. H. Koppens, *Nature* **2012**, *487*, 77.
- [163] Z. Zhang, G. Chen, M. Yang, Y. Ou, L. Luo, D. Lu, E. Zhang, H. Guan, H. Lu, W. Zhu, J. Yu, J. Dong, W. Qiu, Z. Chen, G. Peng, *Nanophotonics* **2020**, *9*, 2387.
- [164] I. Datta, S. H. Chae, G. R. Bhatt, M. A. Tadayon, B. C. Li, Y. L. Yu, C. Park, J. Park, L. Y. Cao, D. N. Basov, J. Hone, M. Lipson, *Nat. Photonics* **2020**, *14*, 256.
- [165] S. Chen, F. Fan, Y. Miao, X. He, K. Zhang, S. Chang, *Nanoscale* **2016**, *8*, 4713.
- [166] Z. Cheng, R. Cao, J. Guo, Y. Yao, K. Wei, S. Gao, Y. Wang, J. Dong, H. Zhang, *Nanophotonics* **2020**, *9*, 1973.
- [167] S. Deckoff-Jones, Y. Wang, H. Lin, W. Wu, J. Hu, *ACS Photonics* **2019**, *6*, 1632.
- [168] F. Xia, T. Mueller, Y.-M. Lin, A. Valdes-Garcia, P. Avouris, *Nat. Nanotechnol.* **2009**, *4*, 839.
- [169] Y. Zhang, T. Liu, B. Meng, X. Li, G. Liang, X. Hu, Q. J. Wang, *Nat. Commun.* **2013**, *4*, 1811.
- [170] M. Breusing, C. Ropers, T. Elsaesser, *Phys. Rev. Lett.* **2009**, *102*, 086809.
- [171] I. H. Lee, D. Yoo, P. Avouris, T. Low, S. H. Oh, *Nat. Nanotechnol.* **2019**, *14*, 313.
- [172] S. Cakmakyapan, P. K. Lu, A. Navabi, M. Jarrahi, *Light: Sci. Appl.* **2018**, *7*, 173.
- [173] M. Engel, M. Steiner, A. Lombardo, A. C. Ferrari, H. v. Löhneysen, P. Avouris, R. Krupke, *Nat. Commun.* **2012**, *3*, 906.
- [174] T. Deng, Z. H. Zhang, Y. X. Liu, Y. X. Wang, F. Su, S. S. Li, Y. Zhang, H. Li, H. J. Chen, Z. R. Zhao, Y. Li, Z. W. Liu, *Nano Lett.* **2019**, *19*, 1494.
- [175] G. Konstantatos, M. Badioli, L. Gaudreau, J. Osmond, M. Bernechea, F. P. G. de Arquer, F. Gatti, F. H. L. Koppens, *Nat. Nanotechnol.* **2012**, *7*, 363.
- [176] X. Liu, T. Galfsky, Z. Sun, F. Xia, E.-C. Lin, Y.-H. Lee, S. Kena-Cohen, V. M. Menon, *Nat. Photonics* **2015**, *9*, 30.
- [177] J. Kwon, Y. K. Hong, G. Han, I. Omkaram, W. Choi, S. Kim, Y. Yoon, *Adv. Mater.* **2015**, *27*, 2224.
- [178] J. Y. Wu, Y. T. Chun, S. P. Li, T. Zhang, J. Z. Wang, P. K. Shrestha, D. P. Chu, *Adv. Mater.* **2018**, *30*, 1705880.
- [179] O. Lopez-Sanchez, D. Lembke, M. Kayci, A. Radenovic, A. Kis, *Nat. Nanotechnol.* **2013**, *8*, 497.
- [180] J. Y. Li, J. F. Han, H. X. Li, X. Y. Fan, K. Huang, *Mater. Sci. Semi-cond. Process.* **2020**, *107*, 104804.
- [181] C. Y. Lan, Z. Y. Zhou, Z. F. Zhou, C. Li, L. Shu, L. F. Shen, D. P. Li, R. T. Dong, S. P. Yip, J. Ho, *Nano Res.* **2018**, *11*, 3371.
- [182] T. J. Wang, K. Andrews, A. Bowman, T. Hong, M. Koehler, J. Q. Yan, D. Mandrus, Z. X. Zhou, Y. Q. Xu, *Nano Lett.* **2018**, *18*, 2766.
- [183] C. J. Zhou, S. Raju, B. Li, M. Chan, Y. Chai, C. Y. Yang, *Adv. Funct. Mater.* **2018**, *28*, 1802954.
- [184] Y. H. Chang, W. Zhang, Y. Zhu, Y. Han, J. Pu, J. K. Chang, W. T. Hsu, J. K. Huang, C. L. Hsu, M. H. Chiu, T. Takenobu, H. Li, C. I. Wu, W. H. Chang, A. T. S. Wee, L. J. Li, *ACS Nano* **2014**, *8*, 8582.

- [185] H. Lee, J. Ahn, S. Im, J. Kim, W. Choi, *Sci. Rep.* **2018**, *8*, 11545.
- [186] T. Y. Su, H. Medina, Y. Z. Chen, S. W. Wang, S. S. Lee, Y. C. Shih, C. W. Chen, H. C. Kuo, F. C. Chuang, Y. L. Chueh, *Small* **2018**, *14*, 1800032.
- [187] C. Y. Chen, H. Qiao, S. H. Lin, C. M. Luk, Y. Liu, Z. Q. Xu, J. C. Song, Y. Z. Xue, D. L. Li, J. Yuan, W. Z. Yu, C. X. Pan, S. P. Lau, Q. L. Bao, *Sci. Rep.* **2015**, *5*, 11830.
- [188] X. Wang, P. Wang, J. Wang, W. Hu, X. Zhou, N. Guo, H. Huang, S. Sun, H. Shen, T. Lin, M. Tang, L. Liao, A. Jiang, J. Sun, X. Meng, X. Chen, W. Lu, J. Chu, *Adv. Mater.* **2015**, *27*, 6575.
- [189] B. C. Deng, R. Frisenda, C. Li, X. L. Chen, A. Castellanos-Gomez, F. N. Xia, *Adv. Opt. Mater.* **2018**, *6*, 1800365.
- [190] Q. S. Guo, A. Pospischil, M. Bhuiyan, H. Jiang, H. Tian, D. Farmer, B. C. Deng, C. Li, S. J. Han, H. Wang, Q. F. Xia, T. P. Ma, T. Mueller, F. N. Xia, *Nano Lett.* **2016**, *16*, 4648.
- [191] M. Engel, M. Steiner, P. Avouris, *Nano Lett.* **2014**, *14*, 6414.
- [192] J. Qiao, X. Kong, Z.-X. Hu, F. Yang, W. Ji, *Nat. Commun.* **2014**, *5*, 4475.
- [193] H. Yuan, X. Liu, F. Afshinmanesh, W. Li, G. Xu, J. Sun, B. Lian, A. G. Curto, G. Ye, Y. Hikita, Z. Shen, S.-C. Zhang, X. Chen, M. Brongersma, H. Y. Hwang, Y. Cui, *Nat. Nanotechnol.* **2015**, *10*, 707.
- [194] S. S. Li, T. Wang, X. S. Chen, W. Lu, Y. Q. Xie, Y. B. Hu, *Nanoscale* **2018**, *10*, 7694.
- [195] M. Long, A. Gao, P. Wang, H. Xia, C. Ott, C. Pan, Y. Fu, E. Liu, X. Chen, W. Lu, T. Nilges, J. Xu, X. Wang, W. Hu, F. Miao, *Sci. Adv.* **2017**, *3*, e1700589.
- [196] X. Wang, Y. Li, L. Huang, X.-W. Jiang, L. Jiang, H. Dong, Z. Wei, J. Li, W. Hu, *J. Am. Chem. Soc.* **2017**, *139*, 14976.
- [197] Z. Zhou, M. Long, L. Pan, X. Wang, M. Zhong, M. Blei, J. Wang, J. Fang, S. Tongay, W. Hu, J. Li, Z. Wei, *ACS Nano* **2018**, *12*, 12416.
- [198] L. J. Pi, C. G. Hu, W. F. Shen, L. Li, P. Luo, X. Z. Hu, P. Chen, D. Y. Li, Z. X. Li, X. Zhou, T. Y. Zhai, *Adv. Funct. Mater.* **2021**, *31*, 2006774.
- [199] L. Li, W. Wang, P. Gong, X. Zhu, B. Deng, X. Shi, G. Gao, H. Li, T. Zhai, *Adv. Mater.* **2018**, *30*, 1706771.
- [200] E. Zhang, Y. Jin, X. Yuan, W. Wang, C. Zhang, L. Tang, S. Liu, P. Zhou, W. Hu, F. Xiu, *Adv. Funct. Mater.* **2015**, *25*, 4076.
- [201] E. Zhang, P. Wang, Z. Li, H. Wang, C. Song, C. Huang, Z.-G. Chen, L. Yang, K. Zhang, S. Lu, W. Wang, S. Liu, H. Fang, X. Zhou, H. Yang, J. Zou, X. Wan, P. Zhou, W. Hu, F. Xiu, *ACS Nano* **2016**, *10*, 8067.
- [202] S. Liu, W. Xiao, M. Zhong, L. Pan, X. Wang, H.-X. Deng, J. Liu, J. Li, Z. Wei, *Nanotechnology* **2018**, *29*, 184002.
- [203] C. Niu, P. M. Buhl, G. Bihlmayer, D. Wortmann, S. Bluegel, Y. Mokrousov, *Nano Lett.* **2015**, *15*, 6071.
- [204] M. Amani, C. L. Tan, G. Zhang, C. S. Zhao, J. Bullock, X. H. Song, H. Kim, V. R. Shrestha, Y. Gao, K. B. Crozier, M. Scott, A. Javey, *ACS Nano* **2018**, *12*, 7253.
- [205] J. Lai, Y. Liu, J. Ma, X. Zhuo, Y. Peng, W. Lu, Z. Liu, J. Chen, D. Sun, *ACS Nano* **2018**, *12*, 4055.
- [206] J. Jiang, Z. K. Liu, Y. Sun, H. F. Yang, C. R. Rajamathi, Y. P. Qi, L. X. Yang, C. Chen, H. Peng, C. C. Hwang, S. Z. Sun, S. K. Mo, I. Vobornik, J. Fujii, S. S. P. Parkin, C. Felser, B. H. Yan, Y. L. Chen, *Nat. Commun.* **2017**, *8*, 13973.
- [207] W. Zhou, J. Chen, H. Gao, T. Hu, S. Ruan, A. Stroppa, W. Ren, *Adv. Mater.* **2019**, *31*, 1804629.
- [208] L. Tong, X. Y. Huang, P. Wang, L. Ye, M. Peng, L. C. An, Q. D. Sun, Y. Zhang, G. M. Yang, Z. Li, F. Zhong, F. Wang, Y. X. Wang, M. Motlag, W. Z. Wu, G. J. Cheng, W. D. Hu, *Nat. Commun.* **2020**, *11*, 2308.
- [209] J. L. Miao, F. J. Zhang, *J. Mater. Chem. C* **2019**, *7*, 1741.
- [210] J. Liu, Y. Xue, Z. Wang, Z. Q. Xu, C. Zheng, B. Weber, J. Song, Y. Wang, Y. Lu, Y. Zhang, Q. Bao, *ACS Nano* **2016**, *10*, 3536.
- [211] H.-C. Cheng, G. Wang, D. Li, Q. He, A. Yin, Y. Liu, H. Wu, M. Ding, Y. Huang, X. Duan, *Nano Lett.* **2016**, *16*, 367.
- [212] Q. Zhang, Y. D. Yin, *ACS Cent. Sci.* **2018**, *4*, 668.
- [213] J. Song, L. Xu, J. Li, J. Xue, Y. Dong, X. Li, H. Zeng, *Adv. Mater.* **2016**, *28*, 4861.
- [214] J. Jeon, H. Choi, S. Choi, J.-H. Park, B. H. Lee, E. Hwang, S. Lee, *Adv. Funct. Mater.* **2019**, *29*, 1905384.
- [215] D. B. Velusamy, J. K. El-Demellawi, A. M. El-Zohry, A. Giugni, S. Lopatin, M. N. Hedhili, A. E. Mansour, E. Di Fabrizio, O. F. Mohammed, H. N. Alshareef, *Adv. Mater.* **2019**, *31*, 1807658.
- [216] W. D. Song, J. X. Chen, Z. L. Li, X. S. Fang, *Adv. Mater.* **2021**, *33*, 2101059.
- [217] J. Yin, Z. Tan, H. Hong, J. Wu, H. Yuan, Y. Liu, C. Chen, C. Tan, F. Yao, T. Li, Y. Chen, Z. Liu, K. Liu, H. Peng, *Nat. Commun.* **2018**, *9*, 3311.
- [218] Y. Y. Niu, D. Wu, Y. Q. Su, H. Zhu, B. Wang, Y. X. Wang, Z. R. Zhao, P. Zheng, J. S. Niu, H. B. Zhou, J. Wei, N. L. Wang, *2D Mater.* **2018**, *5*, 011008.
- [219] T. Fan, Z. Xie, W. Huang, Z. Li, H. Zhang, *Nanotechnology* **2019**, *30*, 114002.
- [220] L. Yao, X. Lou, N. Sui, Q. Liu, Y. Zhang, X. Chi, Z. Kang, Q. Zhou, H. Zhang, Y. Wang, *Opt. Mater.* **2019**, *98*, 109429.
- [221] X. Zhou, X. Hu, S. Zhou, Q. Zhang, H. Li, T. Zhai, *Adv. Funct. Mater.* **2017**, *27*, 1703858.
- [222] H. Xu, L. Hao, H. Liu, S. Dong, Y. Wu, Y. Liu, B. Cao, Z. Wang, C. Ling, S. Li, Z. Xu, Q. Xue, K. Yan, *ACS Appl. Mater. Interfaces* **2020**, *12*, 35250.
- [223] Z. Yang, W. Jie, C.-H. Mak, S. Lin, H. Lin, X. Yang, F. Yan, S. P. Lau, J. Hao, *ACS Nano* **2017**, *11*, 4225.
- [224] M. Yu, H. Li, H. Liu, F. Qin, F. Gao, Y. Hu, M. Dai, L. Wang, W. Feng, P. Hu, *ACS Appl. Mater. Interfaces* **2018**, *10*, 43299.
- [225] H. Huang, X. Ren, Z. Li, H. Wang, Z. Huang, H. Qiao, P. Tang, J. Zhao, W. Liang, Y. Ge, J. Liu, J. Li, X. Qi, H. Zhang, *Nanotechnology* **2018**, *29*, 235201.
- [226] H. Fang, C. Battaglia, C. Carraro, S. Nemsak, B. Ozdol, J. S. Kang, H. A. Bechtel, S. B. Desai, F. Kronast, A. A. Unal, *Proc. Natl. Acad. Sci. USA* **2014**, *111*, 6198.
- [227] J. B. Lee, Y. R. Lim, A. K. Katiyar, W. Song, J. Lim, S. Bae, T. W. Kim, S. K. Lee, J. H. Ahn, *Adv. Mater.* **2019**, *31*, 1904194.
- [228] G. H. Shin, C. Park, K. J. Lee, H. J. Jin, S.-Y. Choi, *Nano Lett.* **2020**, *20*, 5741.
- [229] N. Huo, J. Kang, Z. Wei, S.-S. Li, J. Li, S.-H. Wei, *Adv. Funct. Mater.* **2014**, *24*, 7025.
- [230] A. Varghese, D. Saha, K. Thakar, V. Jindal, S. Ghosh, N. V. Medhekar, S. Ghosh, S. Lodha, *Nano Lett.* **2020**, *20*, 1707.
- [231] Y. Z. Xue, Y. P. Zhang, Y. Liu, H. T. Liu, J. C. Song, J. Sophia, J. Y. Liu, Z. Q. Xu, Q. Y. Xu, Z. Y. Wang, J. L. Zheng, Y. Q. Liu, S. J. Li, Q. L. Bao, *ACS Nano* **2016**, *10*, 573.
- [232] J. Yuan, T. Sun, Z. X. Hu, W. Z. Yu, W. L. Ma, K. Zhang, B. Q. Sun, S. P. Lau, Q. L. Bao, S. H. Lin, S. J. Li, *ACS Appl. Mater. Interfaces* **2018**, *10*, 40614.
- [233] Z. Li, L. Ren, S. Wang, X. Huang, Q. Li, Z. Lu, S. Ding, H. Deng, P. Chen, J. Lin, Y. Hu, L. Liao, Y. Liu, *ACS Nano* **2021**, *15*, 13839.
- [234] T. Mueller, F. Xia, P. Avouris, *Nat. Photonics* **2010**, *4*, 297.
- [235] Y. Liu, R. Cheng, L. Liao, H. Zhou, J. Bai, G. Liu, L. Liu, Y. Huang, X. Duan, *Nat. Commun.* **2011**, *2*, 579.
- [236] M. Furchi, A. Urich, A. Pospischil, G. Lilley, K. Unterrainer, H. Detz, P. Klang, A. M. Andrews, W. Schrenk, G. Strasser, *Nano Lett.* **2012**, *12*, 2773.
- [237] Y. Wang, Y. Zhang, Y. Lu, W. Xu, H. Mu, C. Chen, H. Qiao, J. Song, S. Li, B. Sun, Y.-B. Cheng, Q. Bao, *Adv. Opt. Mater.* **2015**, *3*, 1389.
- [238] Z. Y. Yin, H. Li, H. Li, L. Jiang, Y. M. Shi, Y. H. Sun, G. Lu, Q. Zhang, X. D. Chen, H. Zhang, *ACS Nano* **2012**, *6*, 74.
- [239] D. S. Tsai, K. K. Liu, D. H. Lien, M. L. Tsai, C. F. Kang, C. A. Lin, L. J. Li, J. H. He, *ACS Nano* **2013**, *7*, 3905.
- [240] W. Choi, M. Y. Cho, A. Konar, J. H. Lee, G. B. Cha, S. C. Hong, S. Kim, J. Kim, D. Jena, J. Joo, S. Kim, *Adv. Mater.* **2012**, *24*, 5832.

- [241] J. D. Yao, Z. Q. Zheng, J. M. Shao, G. W. Yang, *Nanoscale* **2015**, 7, 14974.
- [242] J. Xia, X. Huang, L. Z. Liu, M. Wang, L. Wang, B. Huang, D. D. Zhu, J. J. Li, C. Z. Gu, X. M. Meng, *Nanoscale* **2014**, 6, 8949.
- [243] X. Wang, Z. Cheng, K. Xu, H. K. Tsang, J.-B. Xu, *Nat. Photonics* **2013**, 7, 888.
- [244] X. Gan, R.-J. Shiue, Y. Gao, I. Meric, T. F. Heinz, K. Shepard, J. Hone, S. Assefa, D. Englund, *Nat. Photonics* **2013**, 7, 883.
- [245] A. Pospischil, M. Humer, M. M. Furchi, D. Bachmann, R. Guider, T. Fromherz, T. Mueller, *Nat. Photonics* **2013**, 7, 892.
- [246] N. Youngblood, C. Chen, S. J. Koester, M. Li, *Nat. Photonics* **2015**, 9, 247.
- [247] K. Roy, M. Padmanabhan, S. Goswami, T. P. Sai, G. Ramalingam, S. Raghavan, A. Ghosh, *Nat. Nanotechnol.* **2013**, 8, 826.
- [248] W. J. Yu, Y. Liu, H. Zhou, A. Yin, Z. Li, Y. Huang, X. Duan, *Nat. Nanotechnol.* **2013**, 8, 952.
- [249] A. Y. Gao, E. F. Liu, M. S. Long, W. Zhou, Y. Y. Wang, T. L. Xia, W. D. Hu, B. G. Wang, F. Miao, *Appl. Phys. Lett.* **2016**, 108, 223501.
- [250] H. Fang, S. Chuang, T. C. Chang, K. Takei, T. Takahashi, A. Javey, *Nano Lett.* **2012**, 12, 3788.
- [251] K. Xu, D. Chen, F. Yang, Z. Wang, L. Yin, F. Wang, R. Cheng, K. Liu, J. Xiong, Q. Liu, J. He, *Nano Lett.* **2017**, 17, 1065.
- [252] X. Zou, L. Liu, J. Xu, H. Wang, W.-M. Tang, *ACS Appl. Mater. Interfaces* **2020**, 12, 32943.
- [253] L. Xie, M. Z. Liao, S. P. Wang, H. Yu, L. J. Du, J. Tang, J. Zhao, J. Zhang, P. Chen, X. B. Lu, G. L. Wang, G. B. Xie, R. Yang, D. X. Shi, G. Y. Zhang, *Adv. Mater.* **2017**, 29, 1702522.
- [254] A. Nourbakhsh, A. Zubair, R. N. Sajjad, A. K. G. Tavakkoli, W. Chen, S. Fang, X. Ling, J. Kong, M. S. Dresselhaus, E. Kaxiras, K. K. Berggren, D. Antoniadis, T. Palacios, *Nano Lett.* **2016**, 16, 7798.
- [255] X. Xiao, M. Chen, J. Zhang, T. Zhang, L. Zhang, Y. Jin, J. Wang, K. Jiang, S. Fan, Q. Li, *ACS Appl. Mater. Interfaces* **2019**, 11, 11612.
- [256] K. A. Patel, R. W. Grady, K. K. H. Smith, E. Pop, R. Sordan, *2D Mater.* **2020**, 7, 015018.
- [257] S. B. Desai, S. R. Madhupathy, A. B. Sachid, J. P. Llinas, Q. Wang, G. H. Ahn, G. Pitner, M. J. Kim, J. Bokor, C. Hu, H. S. P. Wong, A. Javey, *Science* **2016**, 354, 99.
- [258] B. Radisavljevic, A. Radenovic, J. Brivio, V. Giacometti, A. Kis, *Nat. Nanotechnol.* **2011**, 6, 147.
- [259] H. Wang, L. Yu, Y.-H. Lee, Y. Shi, A. Hsu, M. L. Chin, L.-J. Li, M. Dubey, J. Kong, T. Palacios, *Nano Lett.* **2012**, 12, 4674.
- [260] S. Das, H.-Y. Chen, A. V. Penumatcha, J. Appenzeller, *Nano Lett.* **2013**, 13, 100.
- [261] T. Roy, M. Tosun, J. S. Kang, A. B. Sachid, S. B. Desai, M. Hettick, C. C. Hu, A. Javey, *ACS Nano* **2014**, 8, 6259.
- [262] B. Radisavljevic, M. B. Whitwick, A. Kis, *ACS Nano* **2011**, 5, 9934.
- [263] N. R. Pradhan, D. Rhodes, Y. Xin, S. Memaran, L. Bhaskaran, M. Siddiq, S. Hill, P. M. Ajayan, L. Balicas, *ACS Nano* **2014**, 8, 7923.
- [264] M. Tosun, S. Chuang, H. Fang, A. B. Sachid, M. Hettick, Y. Lin, Y. Zeng, A. Javey, *ACS Nano* **2014**, 8, 4948.
- [265] Y. Du, H. Liu, Y. Deng, P. D. Ye, *ACS Nano* **2014**, 8, 10035.
- [266] S. Das, M. Demarteau, A. Roelofs, *ACS Nano* **2014**, 8, 11730.
- [267] W. Zhu, M. N. Yogeesh, S. Yang, S. H. Aldave, J.-S. Kim, S. Sonde, L. Tao, N. Lu, D. Akinwande, *Nano Lett.* **2015**, 15, 1883.
- [268] H. Wang, X. Wang, F. Xia, L. Wang, H. Jjiang, Q. Xia, M. L. Chin, M. Dubey, S.-j. Han, *Nano Lett.* **2014**, 14, 6424.
- [269] W. C. Tan, Y. Q. Cai, R. J. Ng, L. Huang, X. W. Feng, G. Zhang, Y. W. Zhang, C. A. Nijhuis, X. K. Liu, K. W. Ang, *Adv. Mater.* **2017**, 29, 1700503.
- [270] W. N. Zhu, S. Park, M. N. Yogeesh, K. M. McNicholas, S. R. Bank, D. Akinwande, *Nano Lett.* **2016**, 16, 2301.
- [271] H.-M. Li, D.-Y. Lee, M. S. Choi, D. Qu, X. C.-H. Ra, W. J. Yoo, *Sci. Rep.* **2014**, 4, 4041.
- [272] N. Petrone, T. Cheri, I. Meric, L. Wang, K. L. Shepard, J. Hone, *ACS Nano* **2015**, 9, 8953.
- [273] X. L. Li, X. R. Wang, L. Zhang, S. W. Lee, H. J. Dai, *Science* **2008**, 319, 1229.
- [274] H. Liu, P. D. Ye, *IEEE Electron Device Lett.* **2012**, 33, 546.
- [275] N. R. Pradhan, D. Rhodes, S. Memaran, J. M. Pomirol, D. Smirnov, S. Talapatra, S. Feng, N. Perea-Lopez, A. L. Elias, M. Terrones, P. M. Ajayan, L. Balicas, *Sci. Rep.* **2015**, 5, 8979.
- [276] H. Liu, A. T. Neal, Z. Zhu, Z. Luo, X. Xu, D. Tomanek, P. D. Ye, *ACS Nano* **2014**, 8, 4033.
- [277] Y. R. Shen, *The Principles of Nonlinear Optics*, Wiley, New York **1984**.
- [278] R. W. Boyd, *Nonlinear Optics*, Academic, New York **2008**.
- [279] A. Autere, H. Jussila, Y. Y. Dai, Y. D. Wang, H. Lipsanen, Z. P. Sun, *Adv. Mater.* **2018**, 30, 1705963.
- [280] X. L. Wen, Z. B. Gong, D. H. Li, *InfoMat* **2019**, 1, 317.
- [281] J. W. You, S. R. Bongu, Q. Bao, N. C. Panou, *Nanophotonics* **2019**, 8, 63.
- [282] Q. J. Ma, G. H. Ren, A. Mitchell, J. Z. Ou, *Nanophotonics* **2020**, 9, 2191.
- [283] B. Nabet, *Photodetectors: Materials, Devices and Applications*, Elsevier, London **2015**.
- [284] U. Keller, *Nature* **2003**, 424, 831.
- [285] E. L. Wooten, K. M. Kissa, A. Yi-Yan, E. J. Murphy, D. A. Lafaw, P. F. Hallemeier, D. Maack, D. V. Attanasio, D. J. Fritz, G. J. McBrien, D. E. Bossi, *IEEE J. Sel. Top. Quantum Electron.* **2000**, 6, 69.
- [286] W. R. Zipfel, R. M. Williams, W. W. Webb, *Nat. Biotechnol.* **2003**, 21, 1369.
- [287] N. Kumar, S. Najmaei, Q. N. Cui, F. Ceballos, P. M. Ajayan, J. Lou, H. Zhao, *Phys. Rev. B* **2013**, 87, 161403.
- [288] L. M. Malard, T. V. Alencar, A. P. M. Barboza, K. F. Mak, A. M. de Paula, *Phys. Rev. B* **2013**, 87, 201401.
- [289] Y. L. Li, Y. Rao, K. F. Mak, Y. M. You, S. Y. Wang, C. R. Dean, T. F. Heinz, *Nano Lett.* **2013**, 13, 3329.
- [290] Z. Zhang, L. Zhang, R. Gogna, Z. H. Chen, H. Deng, *Solid State Commun.* **2020**, 322, 114043.
- [291] C. Janisch, Y. X. Wang, D. Ma, N. Mehta, A. L. Elias, N. Perea-Lopez, M. Terrones, V. Crespi, Z. W. Liu, *Sci. Rep.* **2014**, 4, 5530.
- [292] C. T. Le, D. J. Clark, F. Ullah, V. Senthilkumar, J. I. Jang, Y. Sim, M. J. Seong, K. H. Chung, H. Park, Y. S. Kim, *Ann. Phys.* **2016**, 528, 551.
- [293] K. L. Seyler, J. R. Schaibley, P. Gong, P. Rivera, A. M. Jones, S. F. Wu, J. Q. Yan, D. G. Mandrus, W. Yao, X. D. Xu, *Nat. Nanotechnol.* **2015**, 10, 407.
- [294] H. T. Chen, V. Corbolio, A. S. Solntsev, D. Y. Choi, M. A. Vincenti, D. de Ceglia, C. de Angelis, Y. R. Lu, D. N. Neshev, *Light: Sci. Appl.* **2017**, 6, e17060.
- [295] T. K. Fryett, K. L. Seyler, J. J. Zheng, C. H. Liu, X. D. Xu, A. Majumdar, *2D Mater.* **2017**, 4, 015031.
- [296] S. Y. Hong, J. I. Dadap, N. Petrone, P. C. Yeh, J. Hone, R. M. Osgood, *Phys. Rev. X* **2013**, 3, 021014.
- [297] A. Saynatjoki, L. Karvonen, J. Riikonen, W. Kim, S. Mehravar, R. A. Norwood, N. Peyghambarian, H. Lipsanen, K. Kieu, *ACS Nano* **2013**, 7, 8441.
- [298] N. Kumar, J. Kumar, C. Gerstenkorn, R. Wang, H. Y. Chiu, A. L. Smirl, H. Zhao, *Phys. Rev. B* **2013**, 87, 121406.
- [299] C. Beckerleg, T. J. Constant, I. Zeimpekis, S. M. Hornett, C. Craig, D. W. Hewak, E. Hendry, *Appl. Phys. Lett.* **2018**, 112, 011102.
- [300] A. Saynatjoki, L. Karvonen, H. Rostami, A. Autere, S. Mehravar, A. Lombardo, R. A. Norwood, T. Hasan, N. Peyghambarian, H. Lipsanen, K. Kieu, A. C. Ferrari, M. Polini, Z. P. Sun, *Nat. Commun.* **2017**, 8, 893.
- [301] A. Autere, H. Jussila, A. Marini, J. R. M. Saavedra, Y. Y. Dai, A. Saynatjoki, L. Karvonen, H. Yang, B. Amirsolaimani, R. A. Norwood, N. Peyghambarian, H. Lipsanen, K. Kieu, F. J. G. de Abajo, Z. P. Sun, *Phys. Rev. B* **2018**, 98, 115426.
- [302] Q. N. Cui, R. A. Muniz, J. E. Sipe, H. Zhao, *Phys. Rev. B* **2017**, 95, 165406.

- [303] E. Hendry, P. J. Hale, J. Moger, A. K. Savchenko, S. A. Mikhailov, *Phys. Rev. Lett.* **2010**, *105*, 097401.
- [304] D. W. Li, W. Xiong, L. J. Jiang, Z. Y. Xiao, H. R. Golgir, M. M. Wang, X. Huang, Y. S. Zhou, Z. Lin, J. F. Song, S. Ducharme, L. Jiang, J. F. Silvain, Y. F. Lu, *ACS Nano* **2016**, *10*, 3766.
- [305] T. Gu, N. Petrone, J. F. McMillan, A. van der Zande, M. Yu, G. Q. Lo, D. L. Kwong, J. Hone, C. W. Wong, *Nat. Photonics* **2012**, *6*, 554.
- [306] J. Y. Wu, Y. Y. Yang, Y. Qu, L. N. Jia, Y. N. Zhang, X. Y. Xu, S. T. Chu, B. E. Little, R. Morandotti, B. H. Jia, D. J. Moss, *Small* **2020**, *16*, 1906563.
- [307] S. Goossens, G. Navickaite, C. Monasterio, S. Gupta, J. J. Piqueras, R. Perez, G. Burwell, I. Nikitskiy, T. Lasanta, T. Galan, E. Puma, A. Centeno, A. Pesquera, A. Zurutuza, G. Konstantatos, F. Koppens, *Nat. Photonics* **2017**, *11*, 366.
- [308] Y. L. Yin, R. Cao, J. S. Guo, C. Y. Liu, A. Li, X. L. Feng, H. D. Wang, W. Du, A. Qadir, H. Zhang, Y. G. Ma, S. R. R. Gao, Y. Xu, Y. C. Shi, L. M. Tong, D. X. Dai, *Laser Photonics Rev.* **2019**, *13*, 1900032.
- [309] P. Ma, N. Flory, Y. Salamin, B. Baeuerle, A. Emboras, A. Josten, T. Taniguchi, K. Watanabe, L. Novotny, J. Leuthold, *ACS Photonics* **2018**, *5*, 1846.
- [310] S. Deckoff-Jones, H. T. Lin, D. Kita, H. Y. Zheng, D. H. Li, W. Zhang, J. J. Hu, *J. Opt.* **2018**, *20*, 044004.
- [311] J. Q. Wang, Z. Z. Cheng, Z. F. Chen, X. Wan, B. Q. Zhu, H. K. Tsang, C. Shu, J. B. Xu, *Nanoscale* **2016**, *8*, 13206.
- [312] J. F. Gonzalez Marin, D. Unuchek, K. Watanabe, T. Taniguchi, A. Kis, *npj 2D Mater. Appl.* **2019**, *3*, 14.
- [313] Z. Wu, T. Zhang, Y. Chen, Y. Zhang, S. Yu, *Phys. Status Solidi RRL* **2019**, *13*, 1800338.
- [314] H. T. Lin, Y. Song, Y. Z. Huang, D. Kita, S. Deckoff-Jones, K. Q. Wang, L. Li, J. Y. Li, H. Y. Zheng, Z. Q. Luo, H. Z. Wang, S. Novak, A. Yadav, C. C. Huang, R. J. Shiue, D. Englund, T. Gu, D. Hewak, K. Richardson, J. Kong, J. J. Hu, *Nat. Photonics* **2017**, *11*, 798.
- [315] Y. L. Wang, X. Li, Z. B. Jiang, L. Tong, W. T. Deng, X. Y. Gao, X. Y. Huang, H. L. Zhou, Y. Yu, L. Ye, X. Xiao, X. L. Zhang, *Nat. Commun.* **2021**, *12*, 5076.



Junru An is currently a Ph.D. student at Changchun Institute of Optics, Fine Mechanics and Physics under the supervision of Prof. Shaojuan Li. His research interest is mainly focused on the 2D materials for nanoelectronic device application.



Bin Wang received his Ph.D. degree from University of Chinese Academy of Sciences in 2020. He is currently an Assistant Professor at Changchun Institute of Optics, Fine Mechanics and Physics, Chinese Academy of Sciences. His research interests focus on the interaction of plasmons with 2D semiconductor materials.



Shaojuan Li received her Ph.D. degree from Peking University in 2013. She is currently a Professor at Changchun Institute of Optics, Fine Mechanics and Physics, Chinese Academy of Sciences. Her research interests focus on photonics and optoelectronic devices based on 2D materials.



Dabing Li received his Ph.D. degree from University of Chinese Academy of Sciences in 2004. He is currently a Professor at Changchun Institute of Optics, Fine Mechanics and Physics, Chinese Academy of Sciences. His research interests focus on wide-bandgap materials based optoelectronic devices.